Characterizing and Capturing Essential Properties of Materials for the Design of One of NASA's Large Observatories, the James Webb Space Telescope.

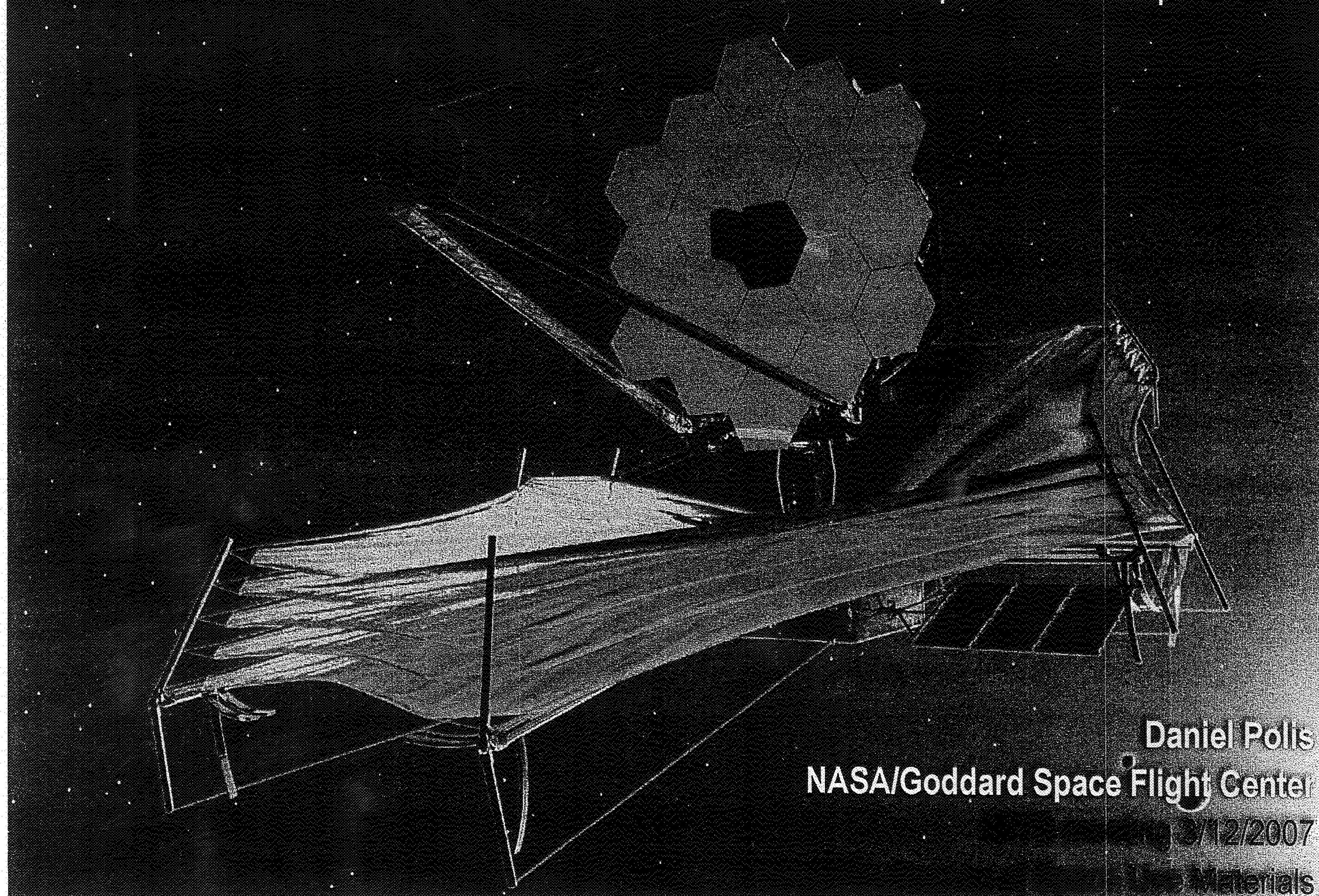

Daniel Polis
NASA/Goddard Space Flight Center
3/12/2007
Materials

Outline

- James Webb Space Telescope (JWST) Overview
- Integrated Science Instrument Module (ISIM) Materials Development
  - Strength
  - Stiffness
  - Thermal Conductivity
  - Thermal Expansion
- Capturing Essential Data

JWST Project Overview

- **Mission Objective: Study the origin and evolution of galaxies, stars and planetary systems by providing Infrared imagery and Spectroscopy**
- **JWST Team:**
  - Mission Lead: GSFC
  - International Collaboration with ESA and CSA
  - Prime Contractor: Northrop Grumman Space Technology with Ball Aerospace as Telescope Subcontractor
  - Ground Segment: Space Telescope Science Institute
  - Science Instrument Providers:
    - Near Infrared Camera (NIRCam): University of Arizona
    - Near Infrared Spectrometer (NIRSpec): ESA
    - Mid Infrared Instrument (MIRI): JPL / ESA
    - Fine Guidance Sensor / Tunable Filter (FGS-TF): CSA
- **Observatory Description:**
  - Deployable telescope w/ 6.5m diameter segmented adjustable primary mirror
  - Cryogenic operating temperature telescope and instruments
  - Deployable Sunshield to allow passive cooling of telescope and instruments
  - Launch in 2013 to Sun-Earth L2
  - 5-year science mission (10-year goal)

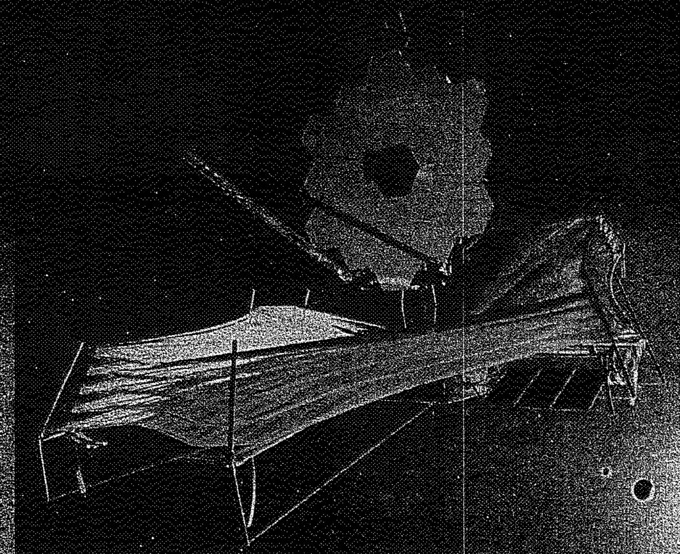

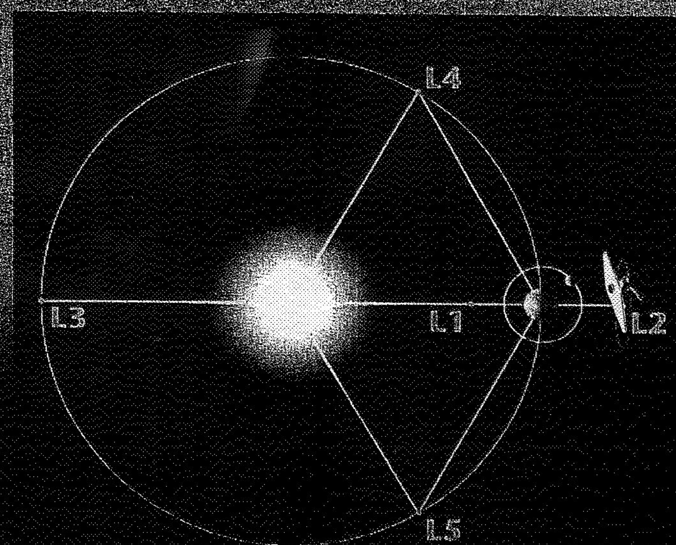

A Brief History of Time

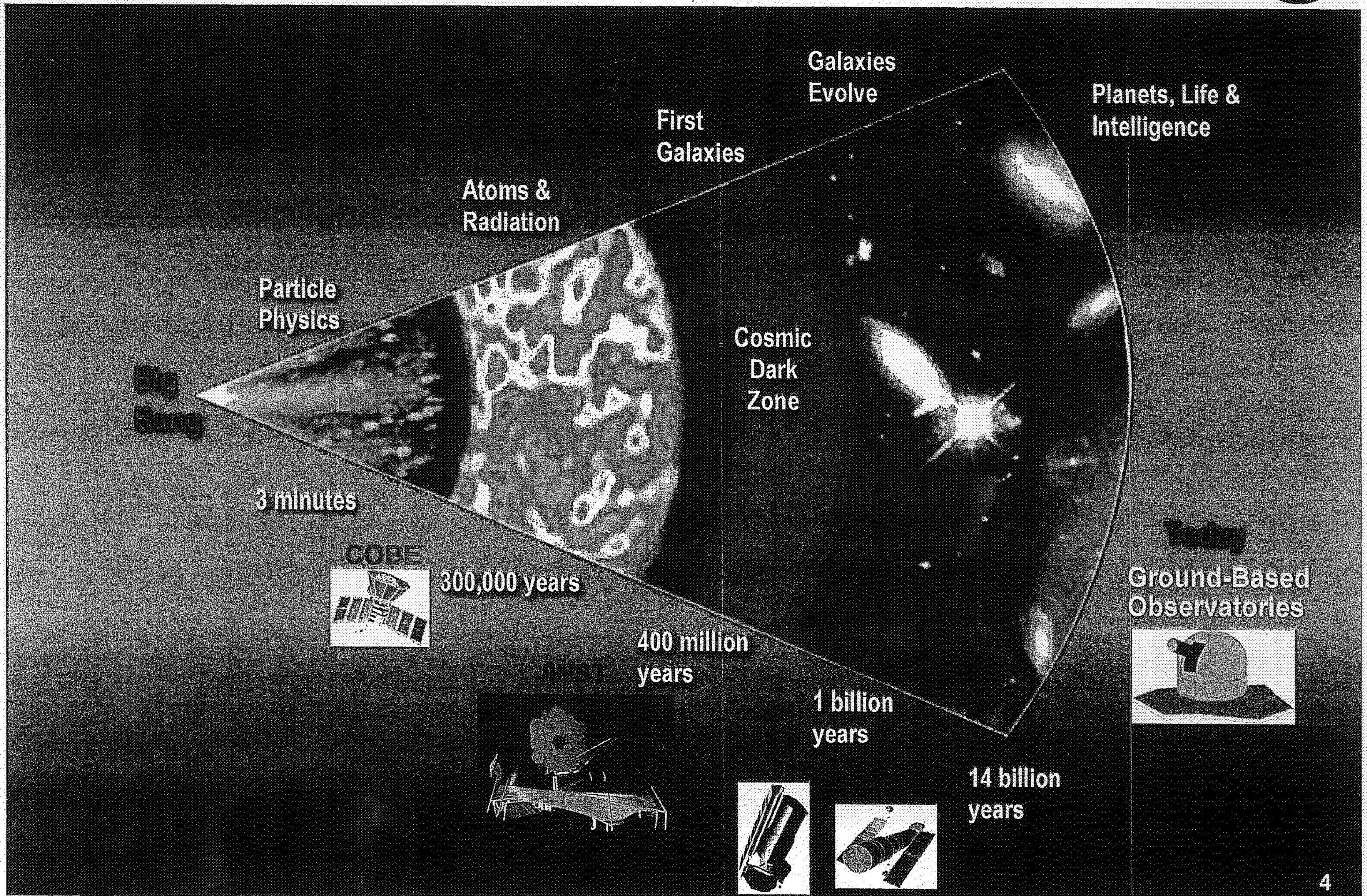

Collecting Infrared Light

- Light from the first galaxies is redshifted from the visible into the infrared.

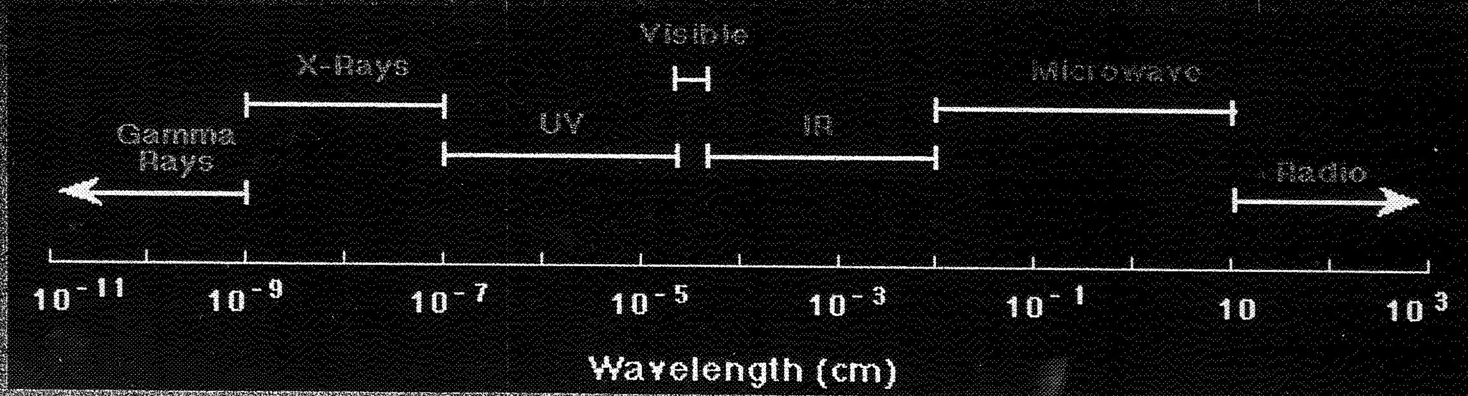

- Infrared is heat radiation
- A telescope must be cold to see in infrared

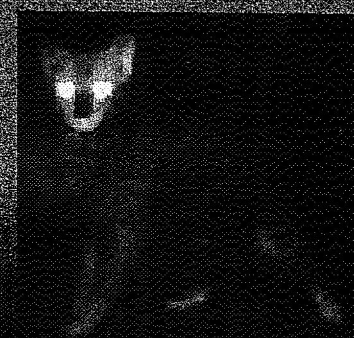

Comparing JWST and HST

- You can fit 7 HST's within the optical area of JWST

2.4 meter diameter

6.5 meter diameter

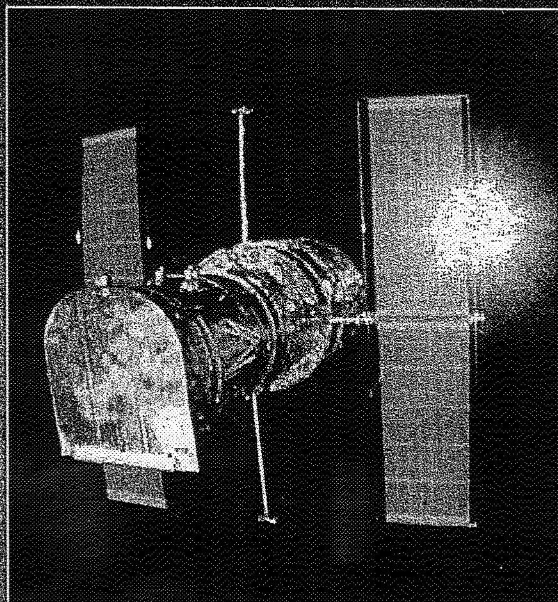

Room Temperature

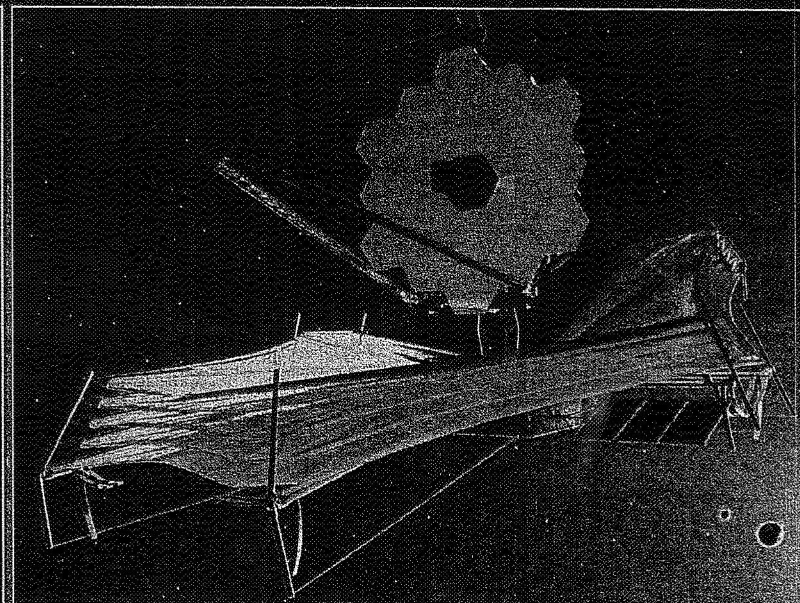

-225° Celsius, 48 Kelvin

- JWST operates in extreme cold to enable sensitive IR collection

Comparing JWST and HST

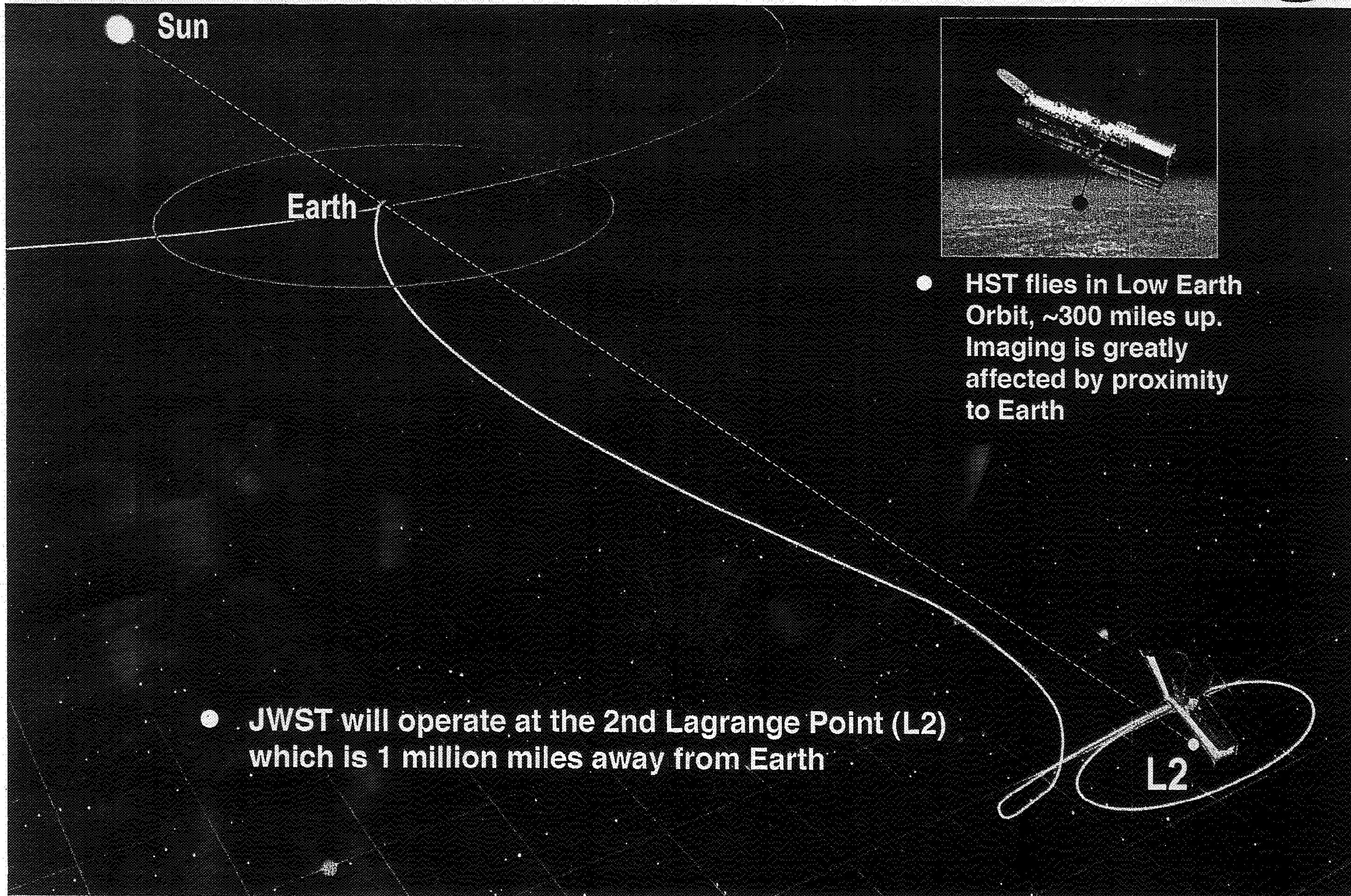

- HST flies in Low Earth Orbit, ~300 miles up. Imaging is greatly affected by proximity to Earth

- JWST will operate at the 2nd Lagrange Point (L2) which is 1 million miles away from Earth

Deployment Sequence

Deployment Animation

JWST Observatory Architecture

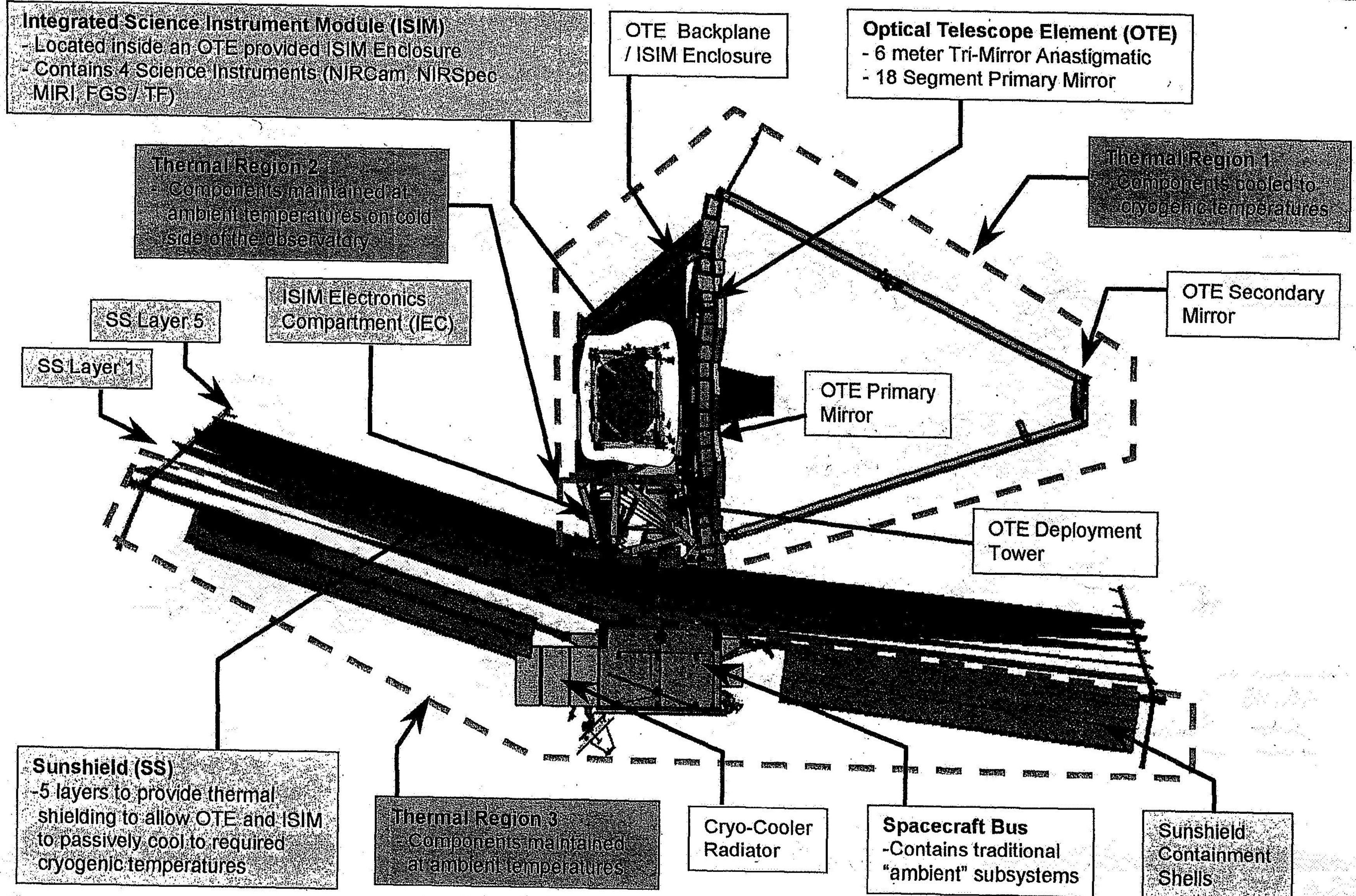

Integrated Science Instrument Module (ISIM)

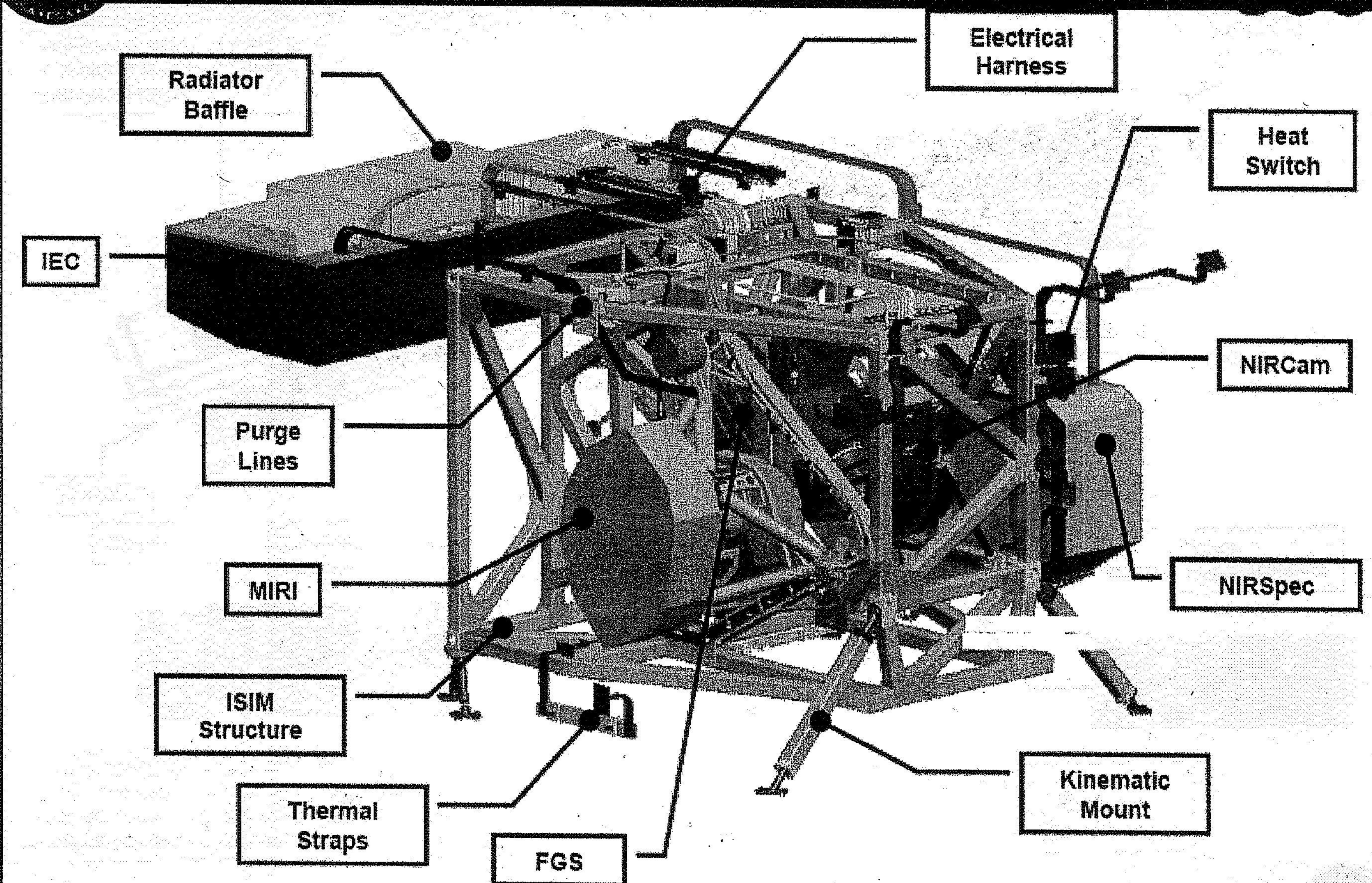

Materials Characterization on the ISIM

1. **Cryogenic Durability** - Optimizing the cryogenic durability of composites by controlling the degree-of-cure (DoC) of the composite matrix.

2. **Stiffness** - Characterizing elastic properties of isotropic materials at cryogenic temperatures using a vibrational technique

3. **Thermal Conductivity** - Characterizing the anisotropy in thermal conductivity from electrical harness insulation in order to understand parasitic heat loads.

4. **Thermal Expansion** - Characterizing the cool down strain from a square composite tube using laser interferometry correlated to finite element modeling.

Cryogenic Durability: Overview

- Prepreg - Hexcel Corporation's M55J/954-6 unidirectional tape, ~0.07 mm thick
- Four laminates were made with the equivalent layup - $[45/0_3/-45/0_2]_{S3}$.
- Autoclave cure profiles:

Laminate	Max 1st ramp rate (°C/min)	1st hold temperature °C (°F)	1st hold time (min)	Max 2nd ramp rate (°C/min)	2nd hold temperature °C (°F)	2nd hold time (min)
A	2	126 (260)	135	-	-	-
B	2	126 (260)	180	-	-	-
C	2	126 (260)	180	2	149 (300)	120
D	2	126 (260)	180	2	176 (350)	120

- All laminates had approximately 60% V_f (1.5% range across the 4 panels)
- Measured DoC, Tg, short beam shear strength, flatwise tensile strength, and microcrack density for each laminate.

Cryogenic Durability: Degree-of-cure and the Effect on T_g

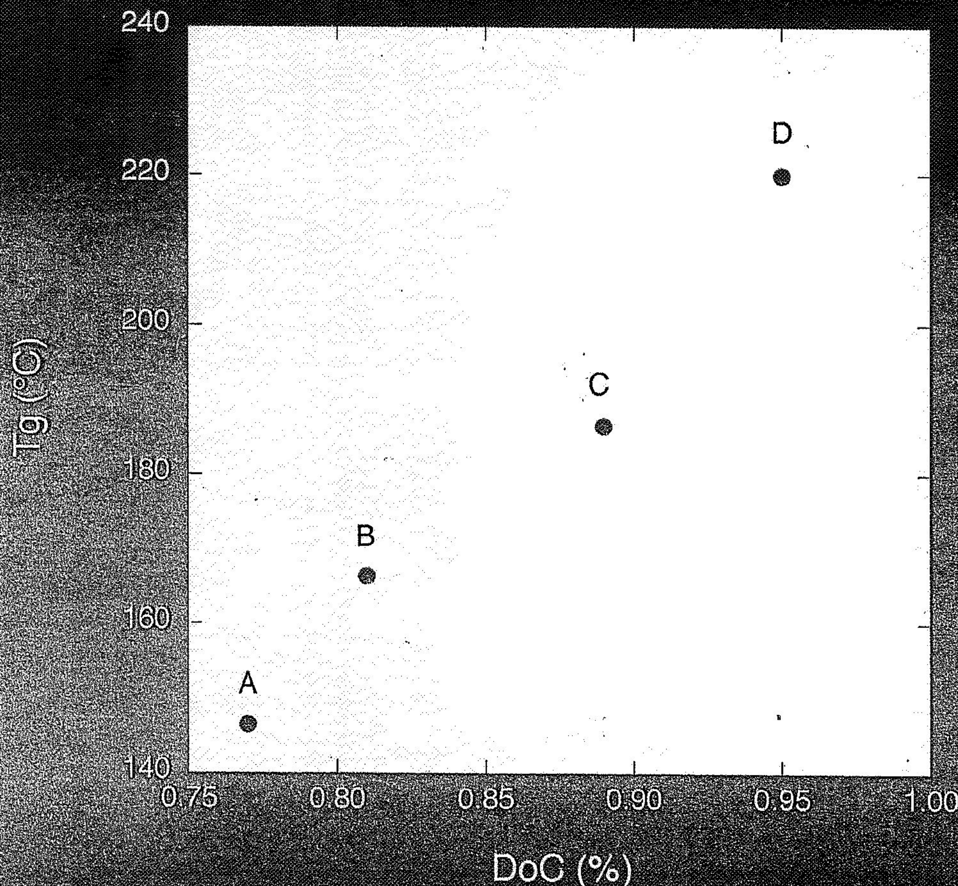

- DoC determination
  - Determined with a differential scanning calorimeter (DSC), using as-received prepreg as the 100% uncured reference.
  - Used a thermogravimetric method to determine the local resin content, in order to normalize the DSC data.
  - 3 sample average for each laminate.

- Tg determination
  - Measured with a dynamic mechanical analyzer.
  - 3-pt bending configuration.
  - 2°C/min heating rate.
  - Report peak in tan Δ (loss modulus/storage modulus)

> 3°C increase in T_g per 1% increase in DoC

Cryogenic Durability: Microcrack Density

- Four 1"x1" samples were cut from each laminate
  - 2 oriented at 0°
  - 2 oriented at 45°
- Microcracks were counted in the 2-3 plane of each lamina.
  - A crack was only counted if it extended the entire thickness of the ply.
- Specimens were cycled between 25 °C to -253 °C (<2 °C/min) and removed at various cycling intervals for microcrack evaluation.

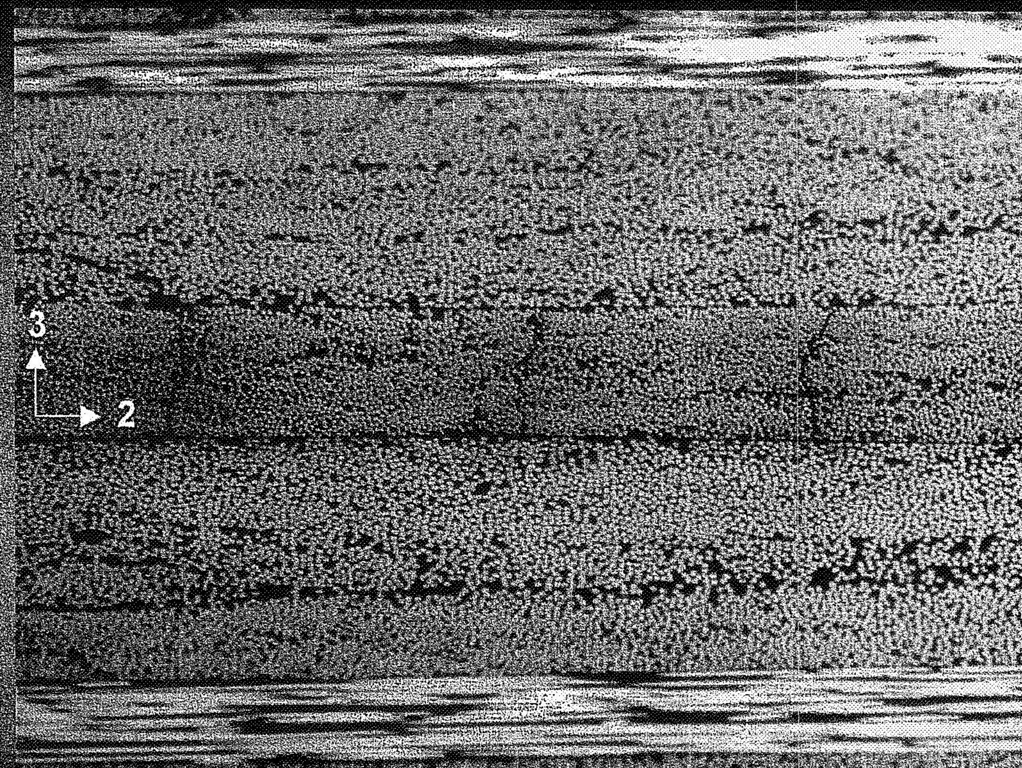

Cryogenic Durability: Microcrack Density (0° Plies)

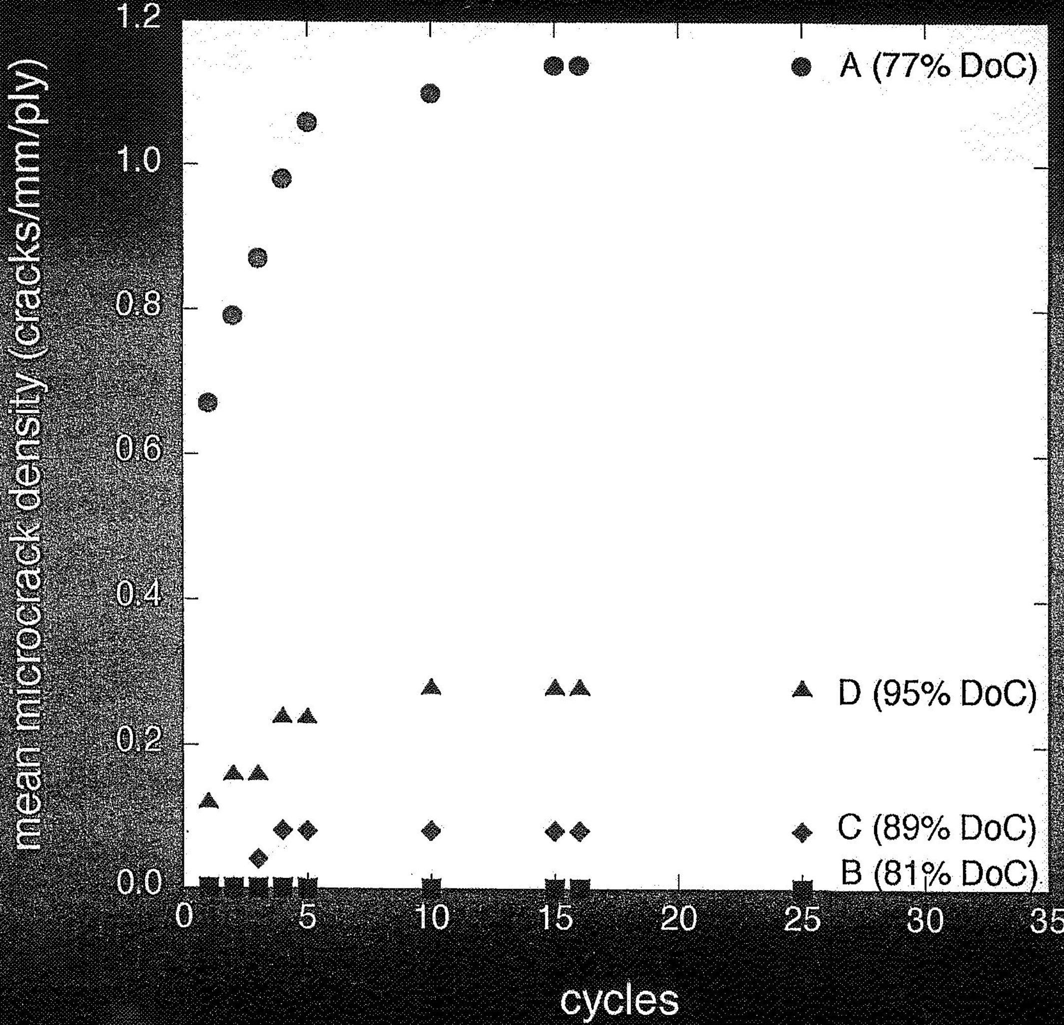

Laminate B shows the lowest microcrack density in the 0° plies

Cryogenic Durability: Microcrack Density (45°/-45° Plies)

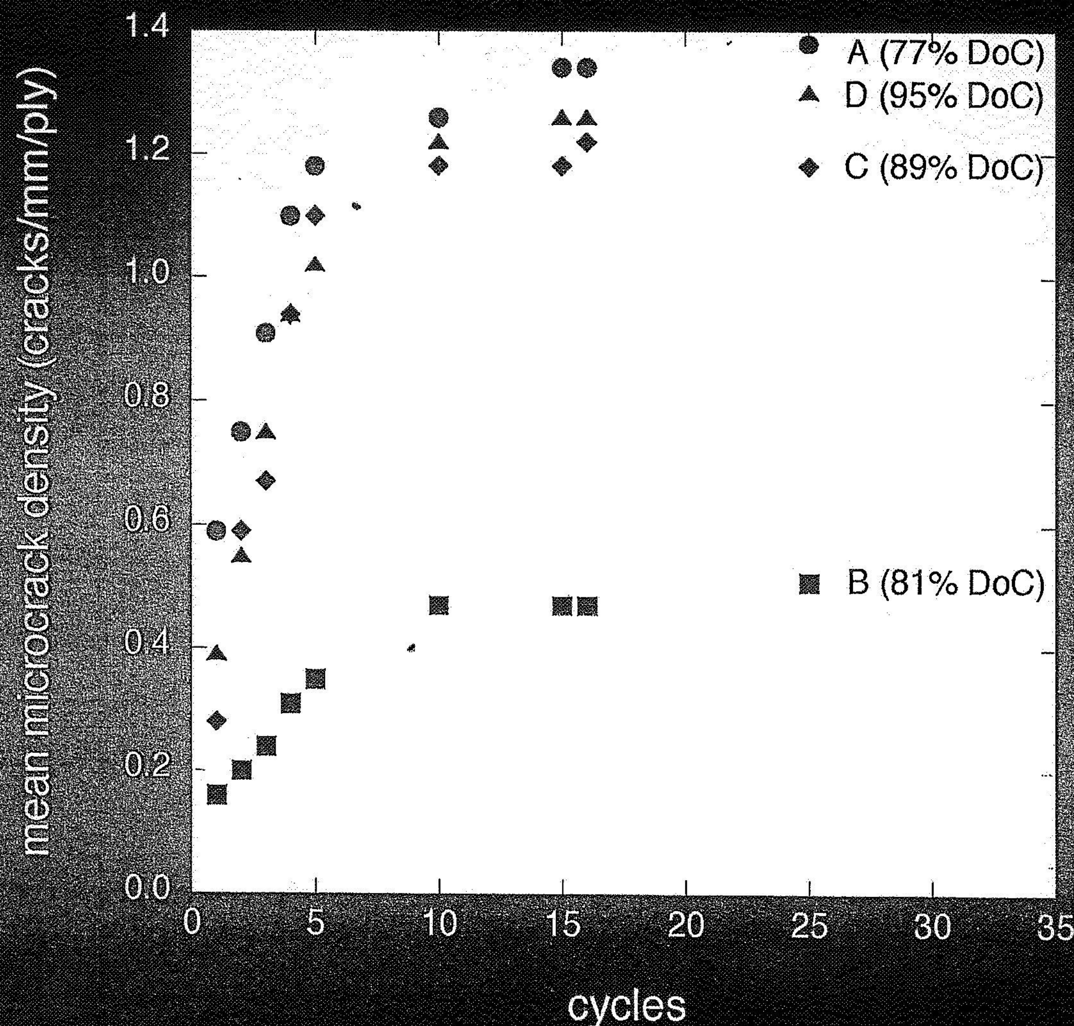

Laminate B shows the lowest microcrack density in the 45° plies

Cryogenic Durability: Flatwise Tensile Strength

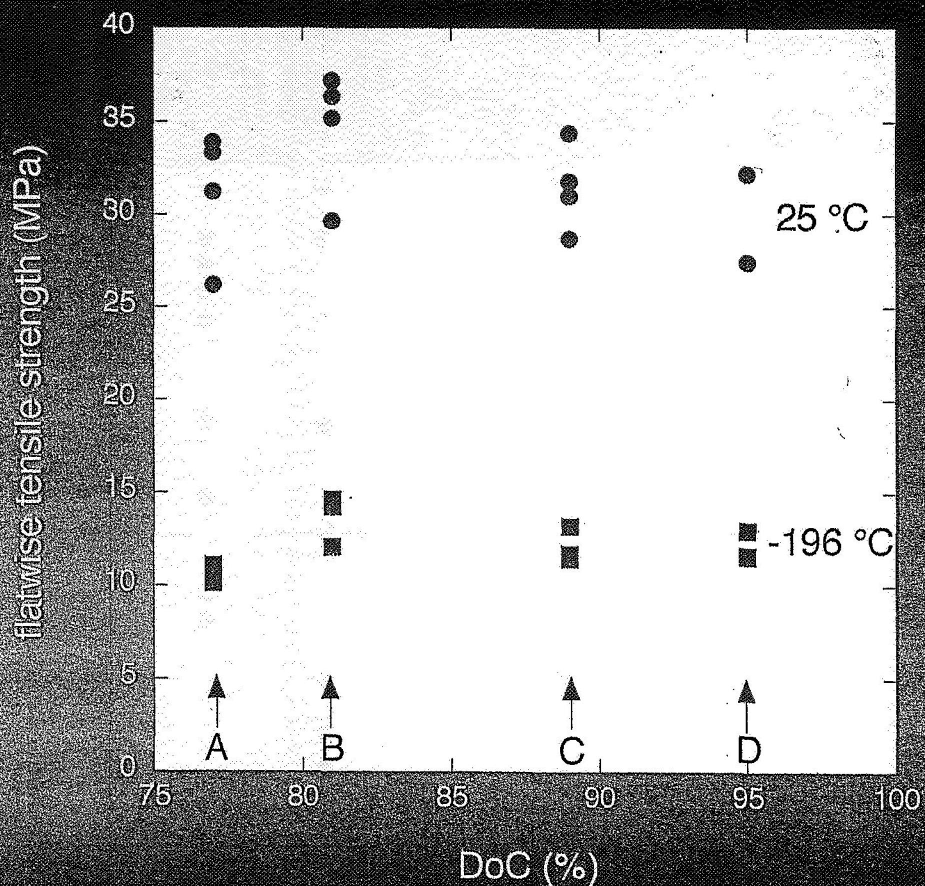

- Specimens (31.8 mm x 31.8 mm) were cycled 20 times between 25 °C to -253 °C prior to bonding.
- Sample were bonded to metal test blocks (25.4 mm x 25.4 mm) for testing at 25 °C (Al blocks) and –196 °C (Invar blocks)
- At 25°C, FEM shows overhang of the laminate (3.2 mm on each side) yields a uniform stress state over block areas.
- At -196 °C, FEM reveals peaking on the order of ~25% above the average failure stress and shear stresses are no longer negligible

Cryogenic Durability: Flatwise Tensile Strength

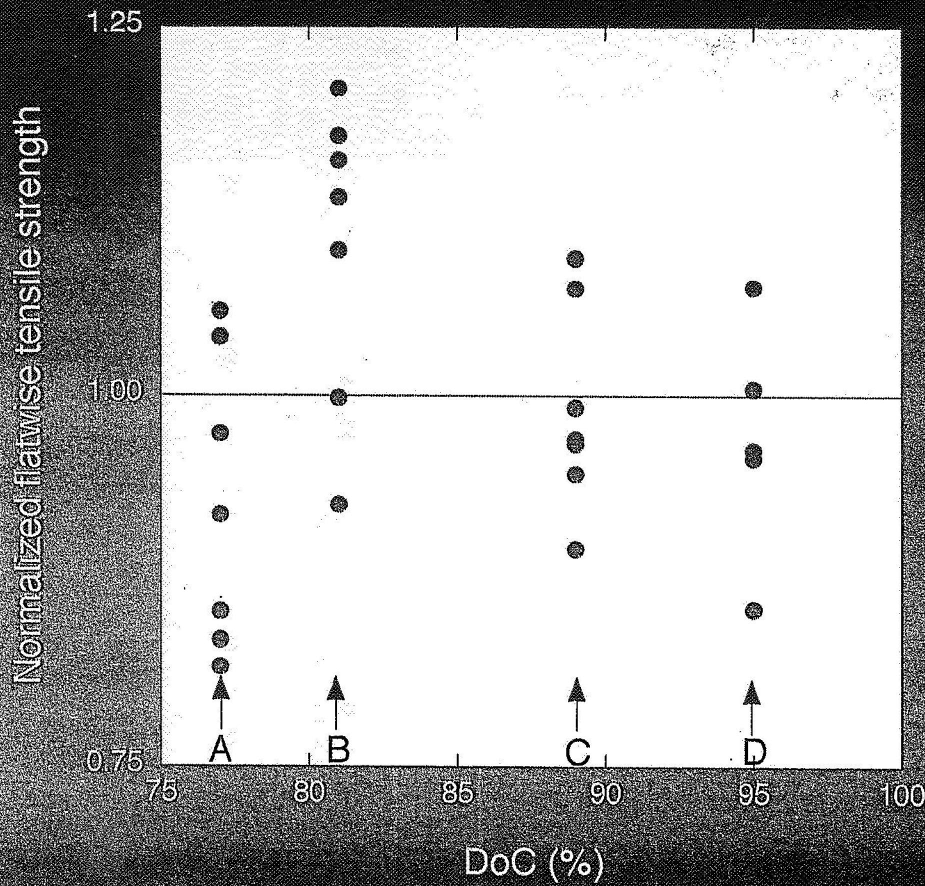

- Combined the 25°C and -196°C data as follows:

$$F^{tu}_{\text{normalized sample X}} = \frac{F^{tu}(\text{sample X tested at } 25\ ^\circ\text{C})}{\text{Average of all samples at } 25\ ^\circ\text{C}}$$

$$F^{tu}_{\text{normalized sample Y}} = \frac{F^{tu}(\text{sample Y tested at } -196\ ^\circ\text{C})}{\text{Average of all samples at } -196\ ^\circ\text{C}}$$

- Mean normalized tensile strengths
  - laminate A = 0.93
  - laminate B = 1.10
  - laminate C = 0.99
  - laminate D = 0.97
- Pooled standard dev = 0.09

Laminate B shows improved flatwise tensile strength relative to the other laminates following cryogenic cycling

Cryogenic Durability: Short-beam Shear Strength

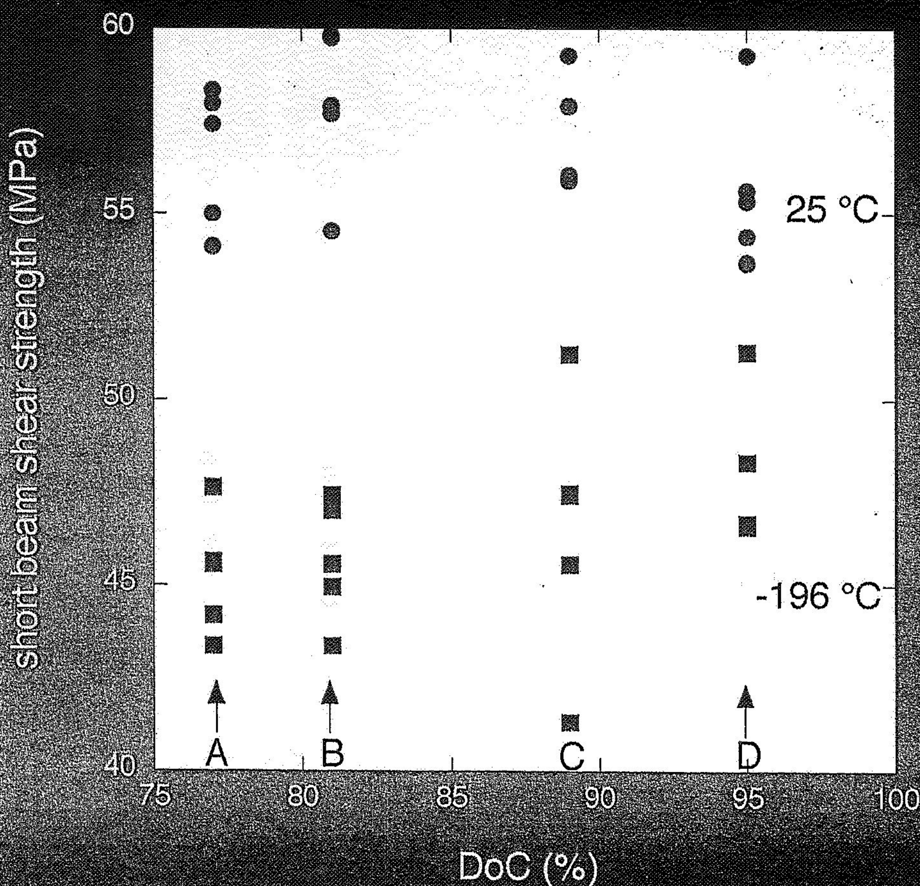

- Tested in accordance with ASTM D 2344, "Standard Test Method for Short-Beam Strength of Polymer Matrix Composite Materials and Their Laminates."

- Nominal specimen dimensions 3 mm x 6 mm x 18 mm.

- Loading rate of 1.27 mm/min.

Cryogenic Durability: Short-beam Shear Strength

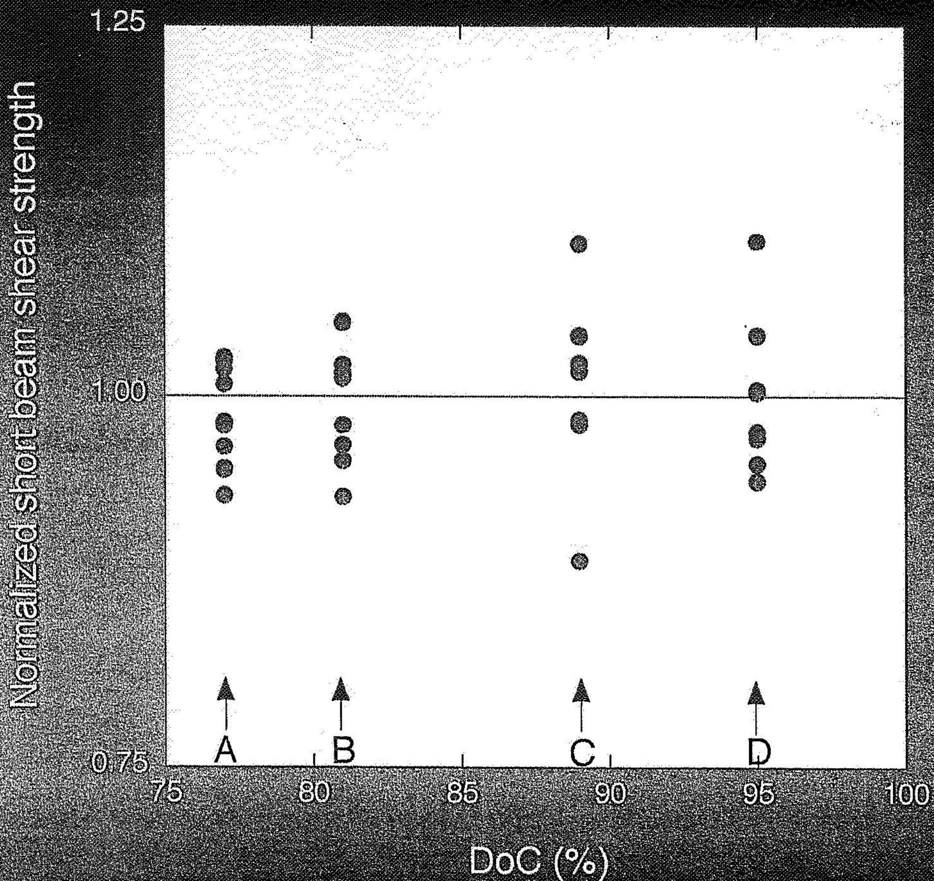

- Combined the 25°C and -196°C data as follows:

$$F^{tu}_{\text{normalized sample X}} = \frac{F^{tu}(\text{sample X tested at } 25\ ^\circ\text{C})}{\text{Average of all samples at } 25\ ^\circ\text{C}}$$

$$F^{tu}_{\text{normalized sample Y}} = \frac{F^{tu}(\text{sample Y tested at } -196\ ^\circ\text{C})}{\text{Average of all samples at } -196\ ^\circ\text{C}}$$

- Mean normalized shear strengths
  - laminate A = 0.98
  - laminate B = 1.00
  - laminate C = 1.01
  - laminate D = 1.01
- Pooled standard dev = 0.05

Laminate short-beam shear strength is not sensitive to DoC following cryogenic cycling

Cryogenic Durability: Summary

- The occurrence of a maximum in the flatwise tensile strength and (microcrack density)$^{-1}$ versus DoC indicate two competing effects

- The competing effects may be resin strength and the cool down residual stress from the cure temperature.

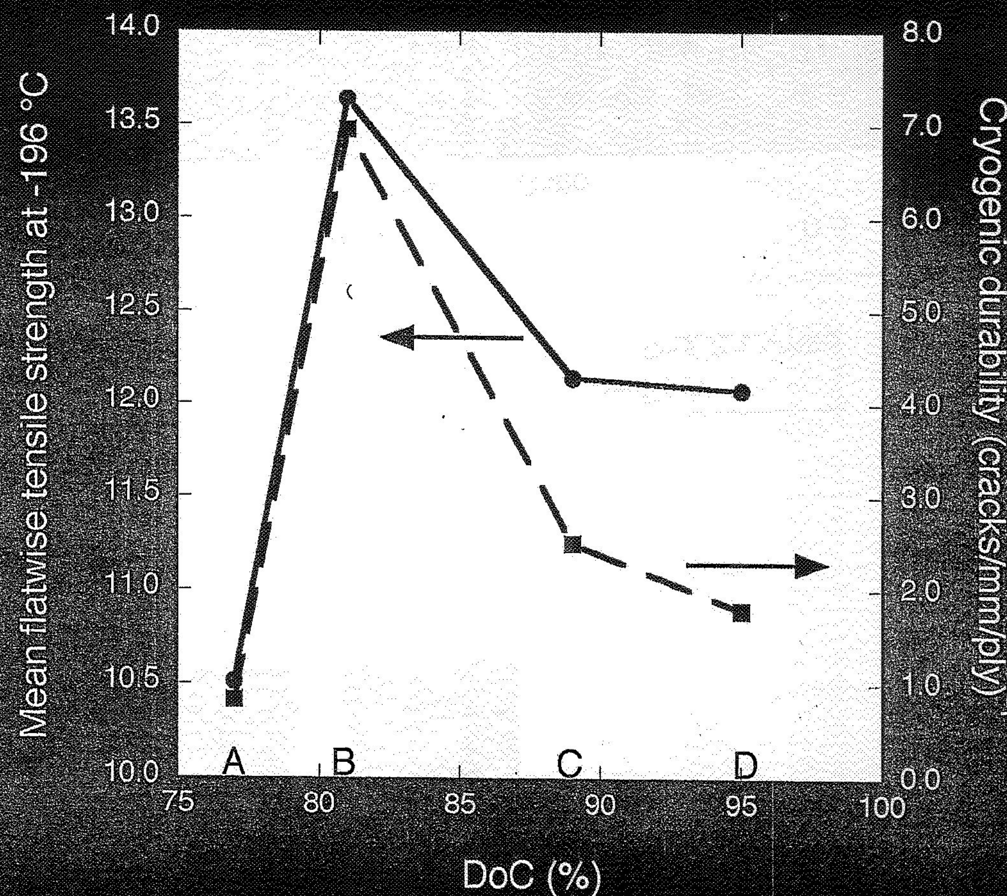

Mechanical and physical properties can be optimized for cryogenic temperatures by controlling the degree-of-cure.

Stiffness: Vibrating Plate Overview

Principles: The ratio of resonant frequencies of O and X modes of a square plate is only a function of Poisson's Ratio of the plate material. Young's modulus and shear modulus of the material can be determined by the Poisson's Ratio and the resonant frequencies.

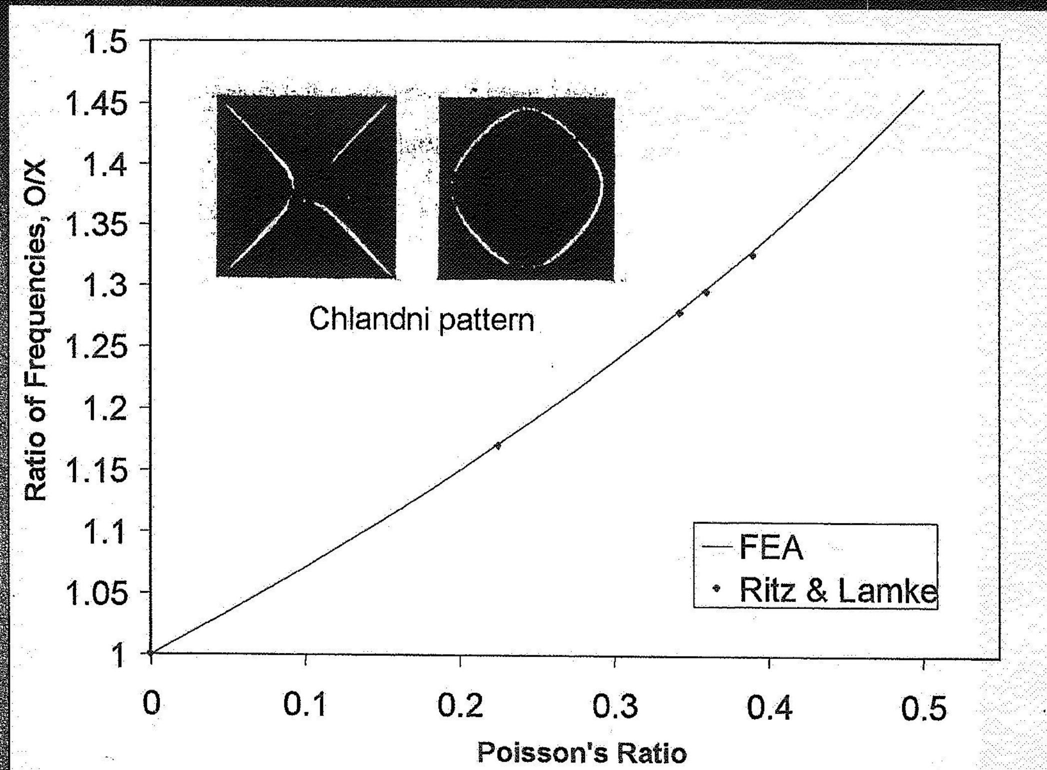

Advantages: Measurement can be very accurate at any temperatures. All of the elastic properties, E, G and ν, can be determined simultaneously by single specimen test.

Stiffness: Experimental Setup

Square plate sample is simply supported at four node points, which are shared by the two vibration modes. Magnetic transducers are used for excitation and detection.

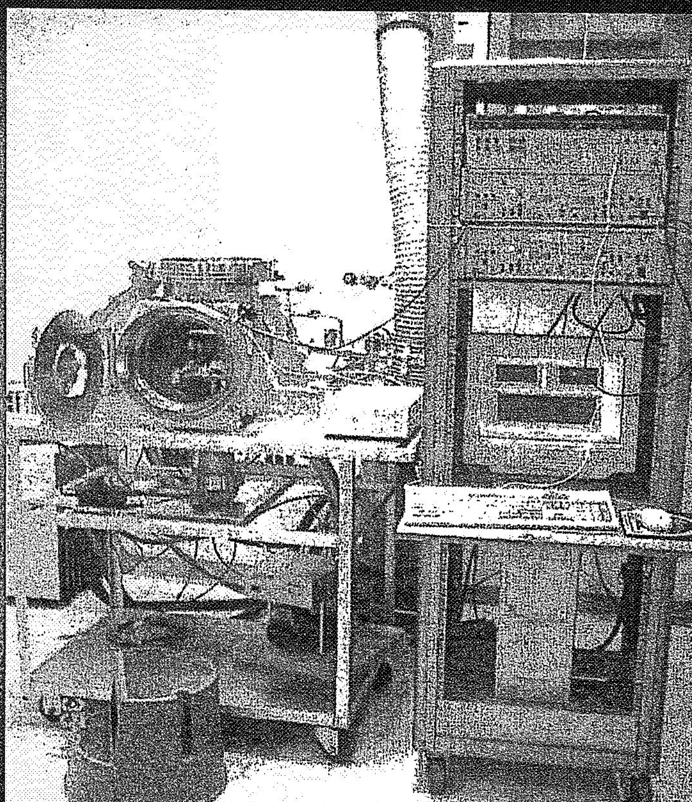

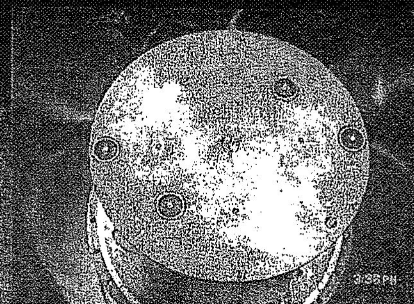

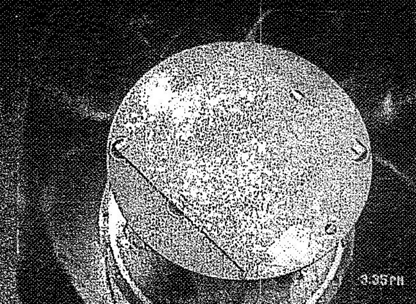

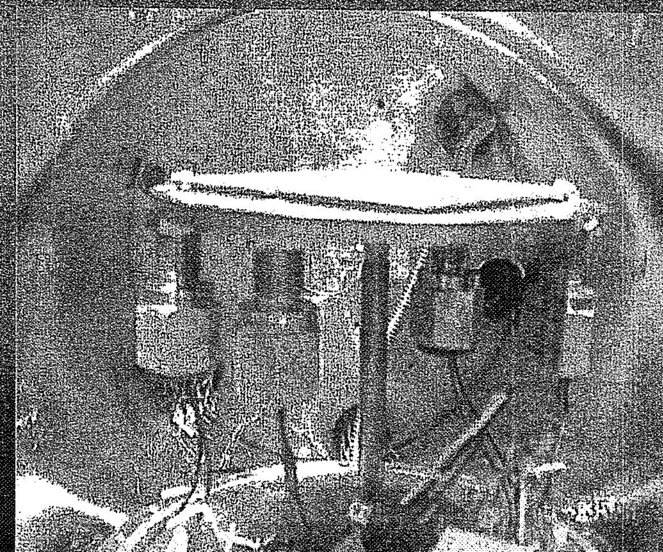

Stiffness: Invar 36 Elastic Properties

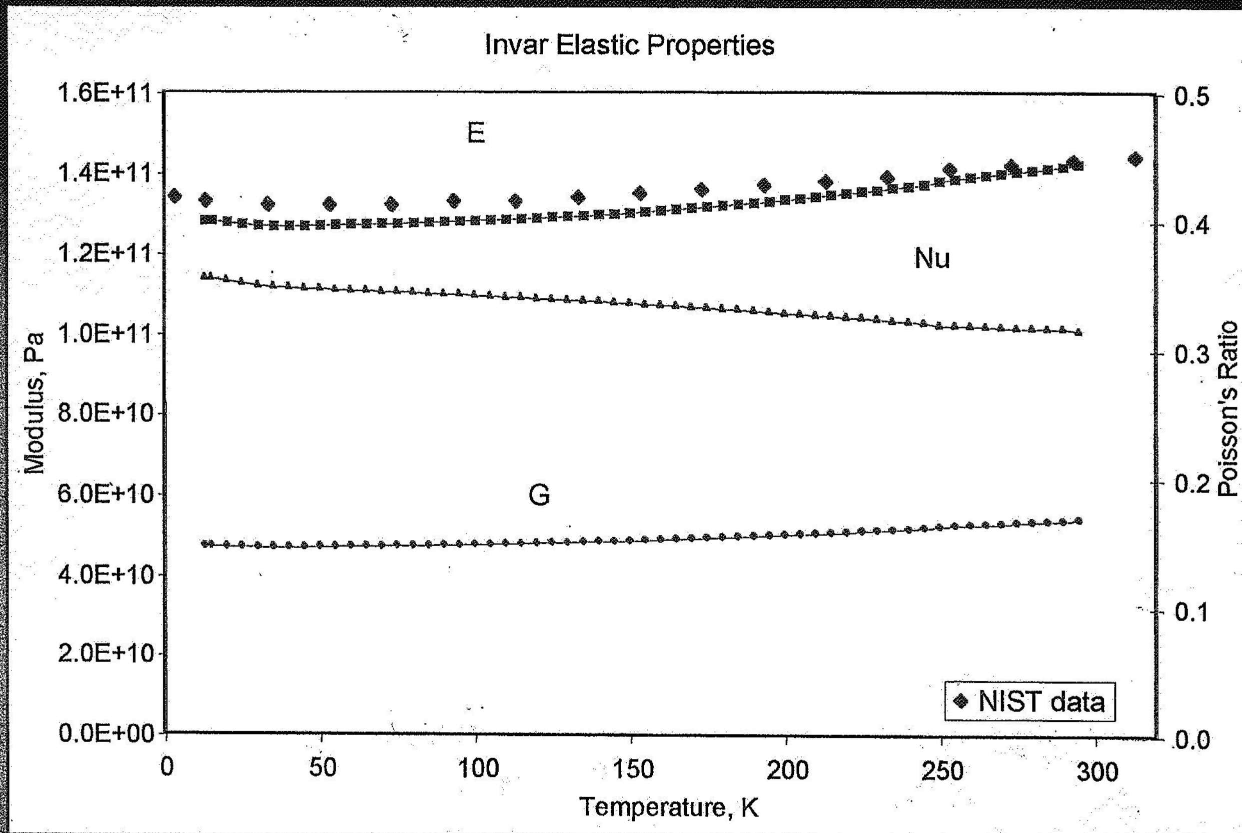

Close agreement with NIST data for Invar 36
- small deviation is due to NIST assumption of constant ν

Stiffness: Epoxy Elastic Properties

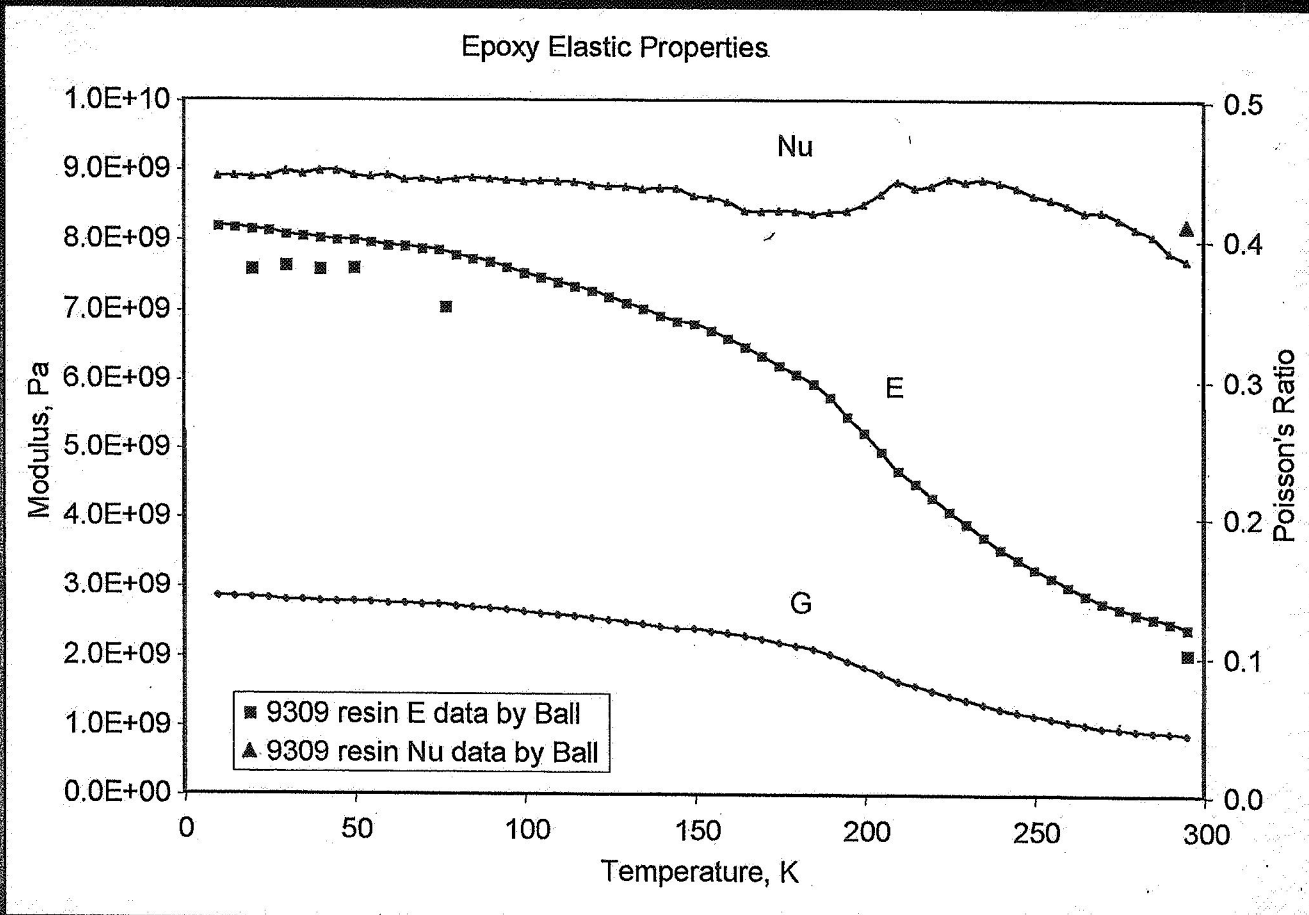

E, *G* and *ν* simultaneously determined as a function of temperature, which has been incorporated into the distortion and strength analysis of the ISIM structure.

Thermal Conductivity: Anisotropy Determination

- Thermal testing of an instrument harness indicated that the conductance was significantly higher than expected.

- One hypothesis for the high conductance was due to anisotropic thermal conductivity from the jacket materials. More specifically, a through-the-thickness conductivity was used in the thermal model, but the conductance measurement of the harness is driven by the axial properties.

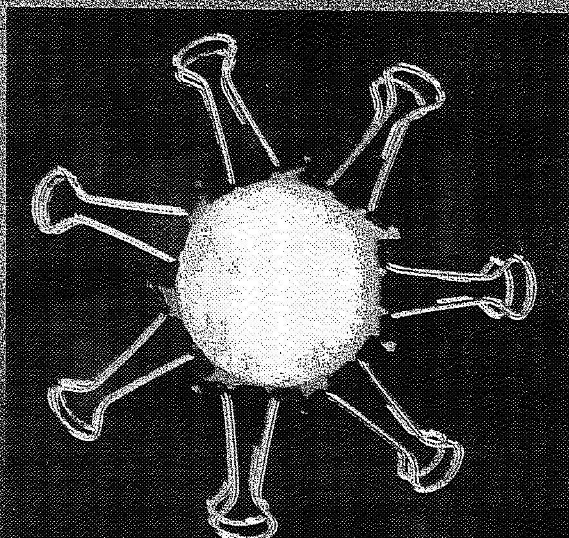

- A piece of the outer jacket (ePTFE) was removed for testing.

- The 0.7 mm thick film was clamped between two copper gaskets to get a uniform boundary condition.

Thermal Conductivity: Experimental Overview

- Test method follows a similar approach described by Cernuschi et. al.[1], in which a film is heated by a Gaussian heat source on one side and an IR camera monitors the time evolution of the temperature profile on the other side.

- The ratio of thermal diffusivity along the harness direction (X) relative to that transverse to the harness (Y) is determined by following the time evolution of the temperature maps along these respective directions.

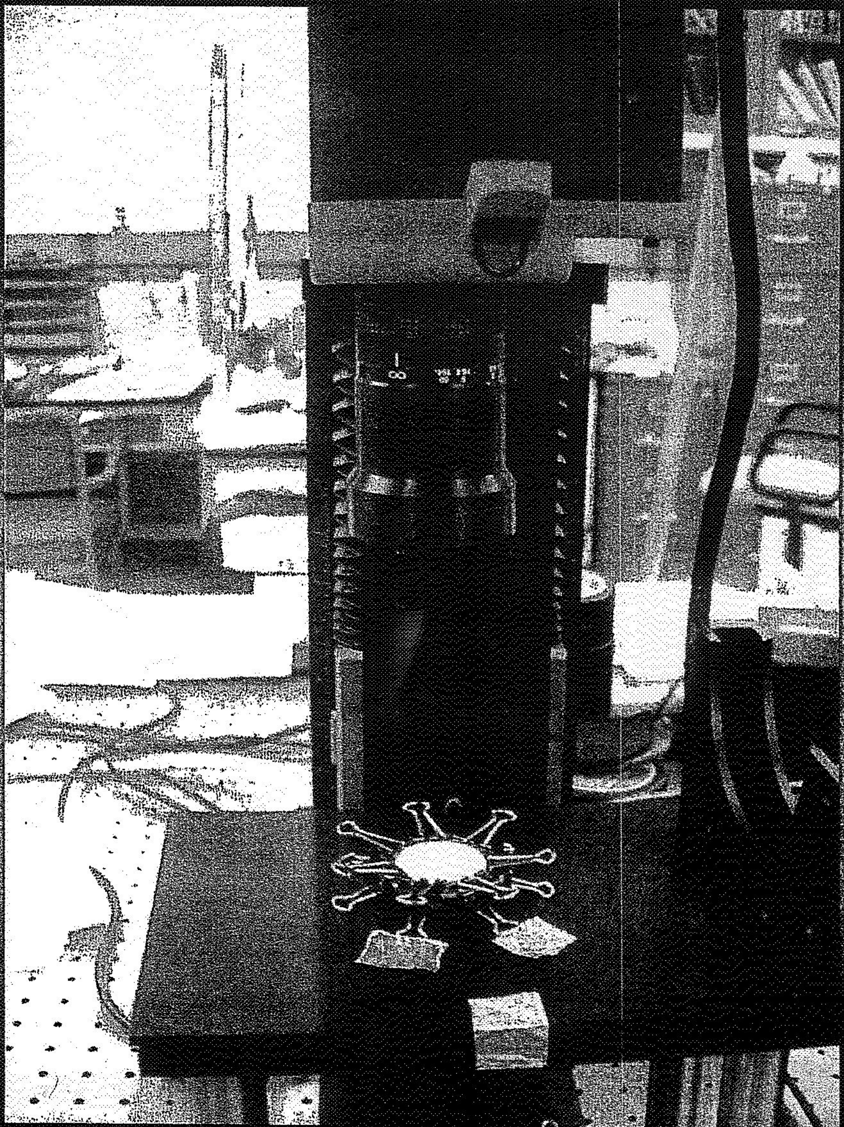

1. Cernuschi et. al. "In-plane thermal diffusivity evaluation by infrared thermography." Review of Scientific Instruments, 72(10), p3988-399, 2001.

Thermal Conductivity: Data Reduction

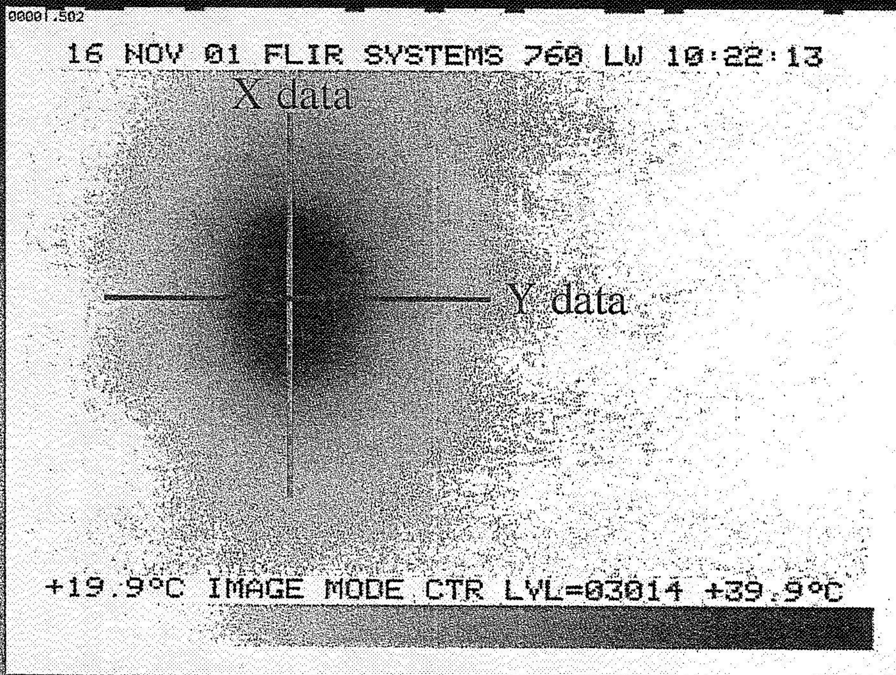

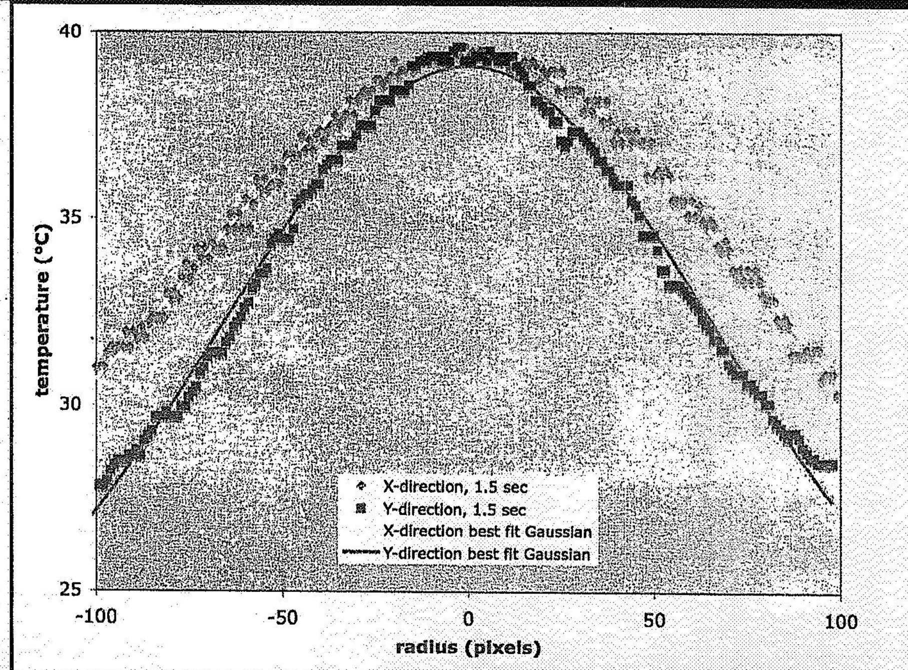

- Best fit X and Y data to Gaussian : $(A/B)*\exp(-2r^2/B)+C$
  - where the shape factor, $B = R^2 + 8\alpha t$
  - r = radial coordinate, R = radius of heat source, α = thermal diffusivity, t = time, A and C are fitting factors
- Plot B versus t, for both X and Y data.
  - The ratio of the slopes is the thermal diffusivity ratio
  - The thermal diffusivity ratio = thermal conductivity ratio, because the heat capacity and density are equivalent.

Thermal Conductivity: Results

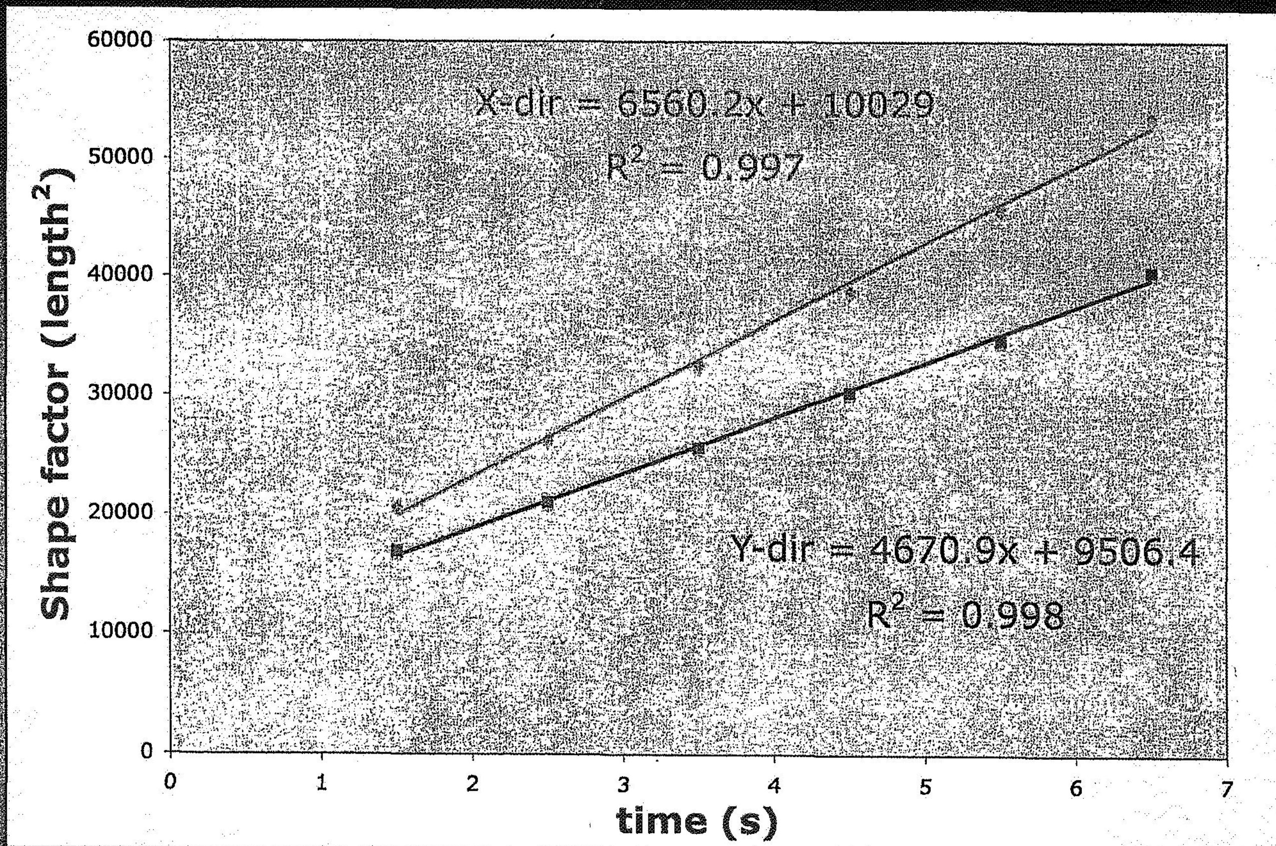

Thermal conductivity ratio (X/Y) = 1.4 (6560/4671)

Thermal Conductivity: Morphology Correlation

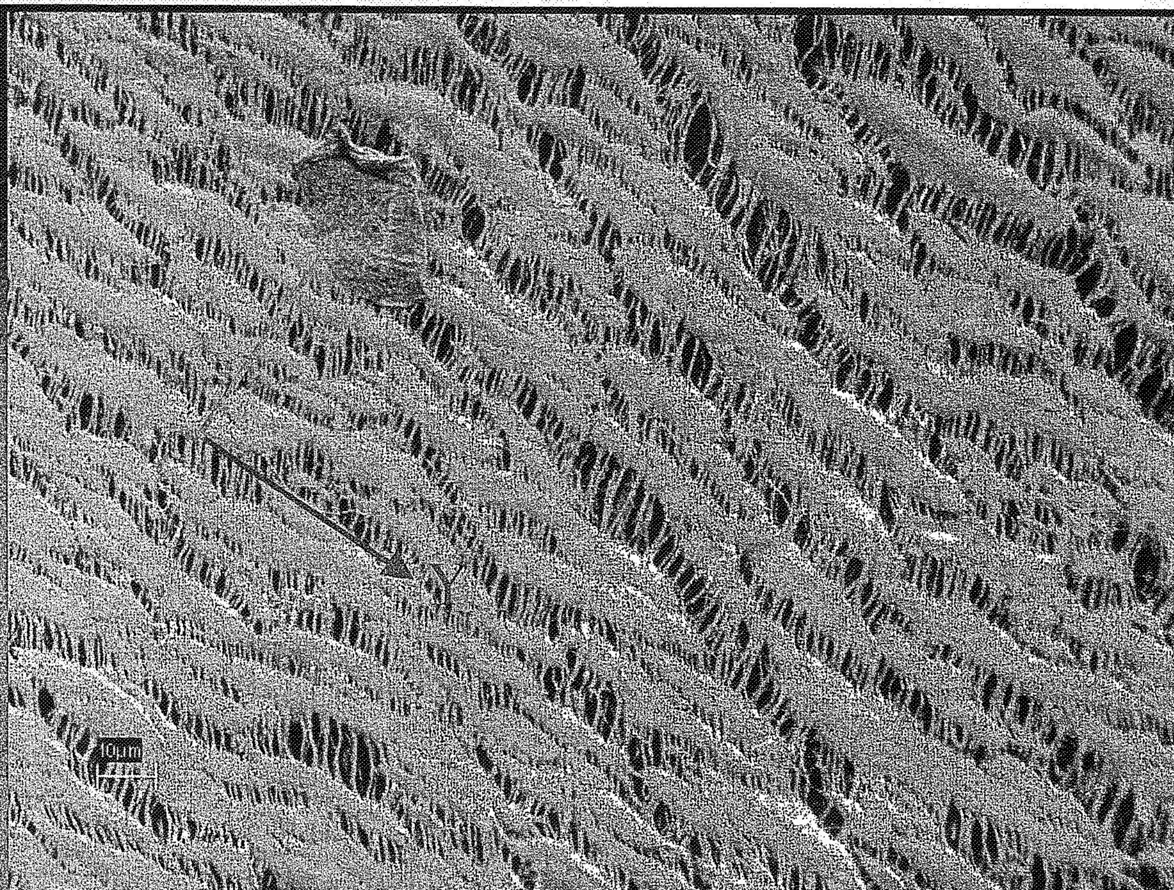

- SEM shows fibrils with uniaxial orientation along the X-dir, consistent with thermal and mechanical data.
- Expect properties in Z-dir to be similar to that in Y-dir

Potentials for reducing harness axial conductance

- Use the same material rotated 90° with respect to the harness axis if the sheet material is available is wide enough form.
- Use a tape wrap/fuse approach to achieve properties similar to Y properties.
- Use biaxially expanded ePTFE product to achieve an average of X and Y properties

Thermal Expansion: Overview

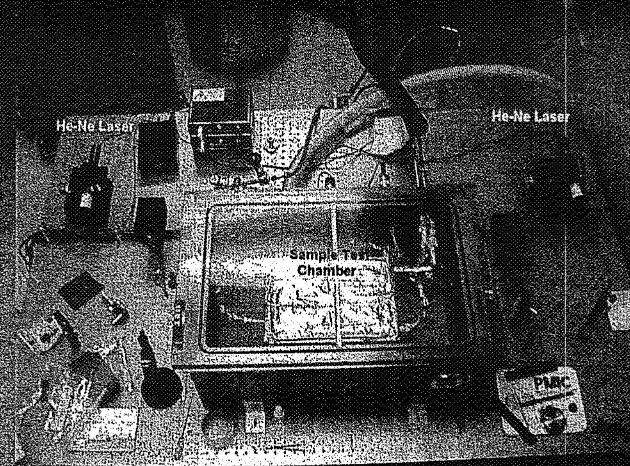

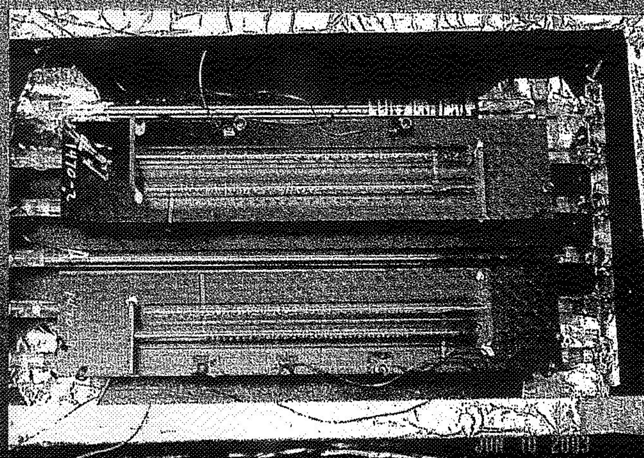

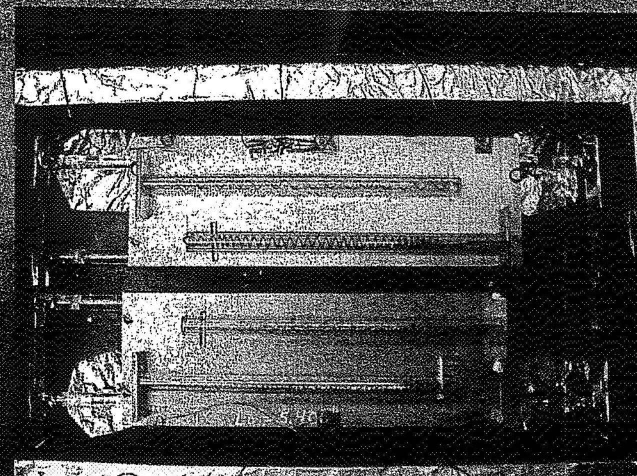

Thermal Expansion: Low Expansion Materials

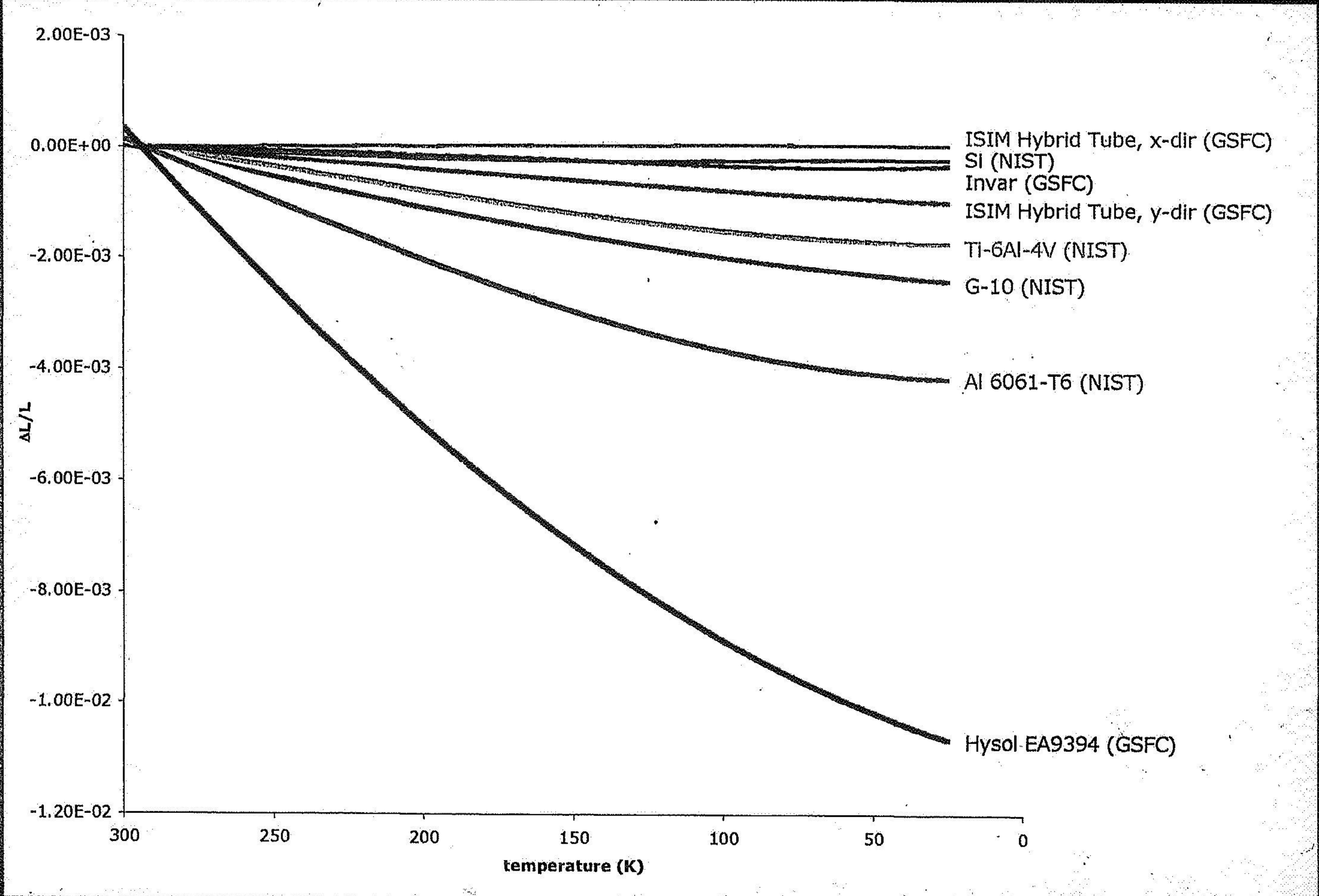

ISIM Composites expand axially by only ~70 ppm over the entire cool down, as compared to Invar, which contracts ~400 ppm.

Thermal Expansion: Facility Calibration

Calibrate facility using Single Crystal Silicon

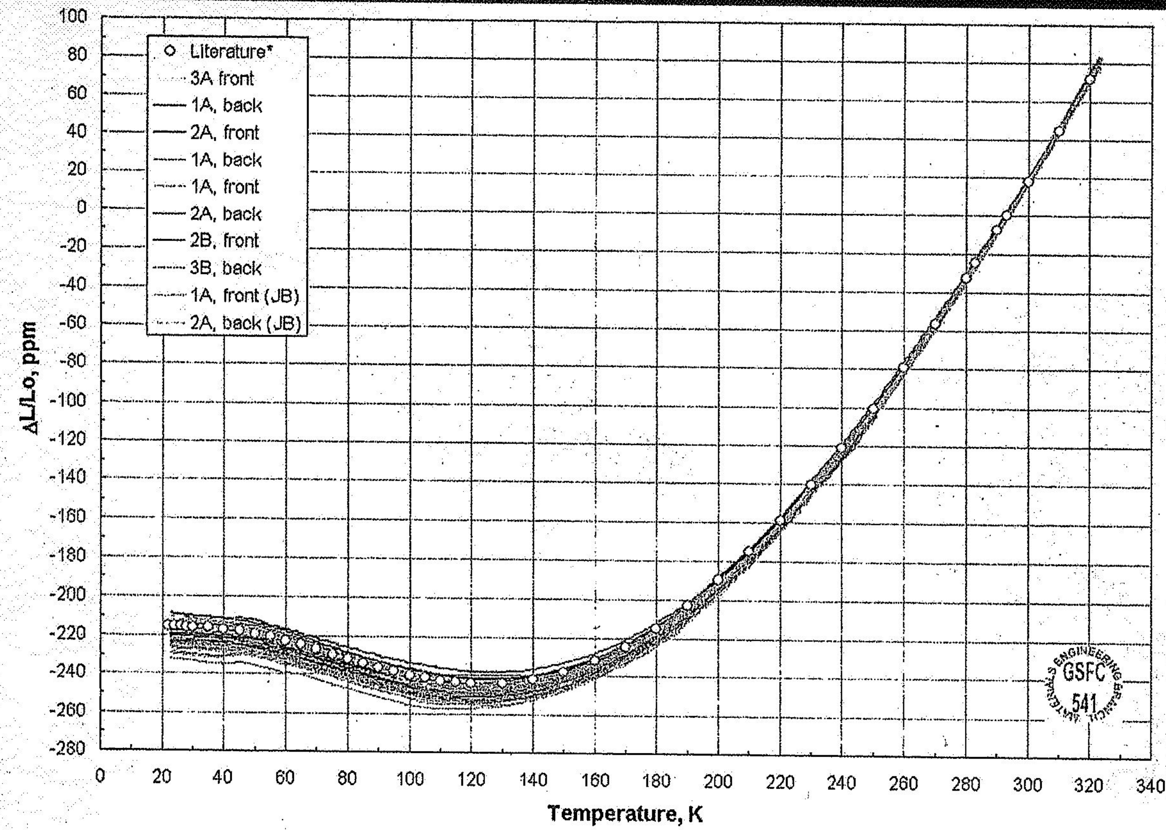

* K.G. Lyon, G.L. Salinger, C.A. Swenson, G.K. White, "Linear Thermal Expansion Measurements on Silicon from 6 to 340K", J. Appl. Phys., Vol. 48, No. 3, 865-868(1977)

30 K analysis

- < 5 ppm bias observed relative to NIST data.
- Standard error for the cool down strain < 5.5 ppm
- In order to resolve differences that are less than are on the order of 10 ppm, need to average the response of several samples

Thermal Expansion: The effect of a closed form shape

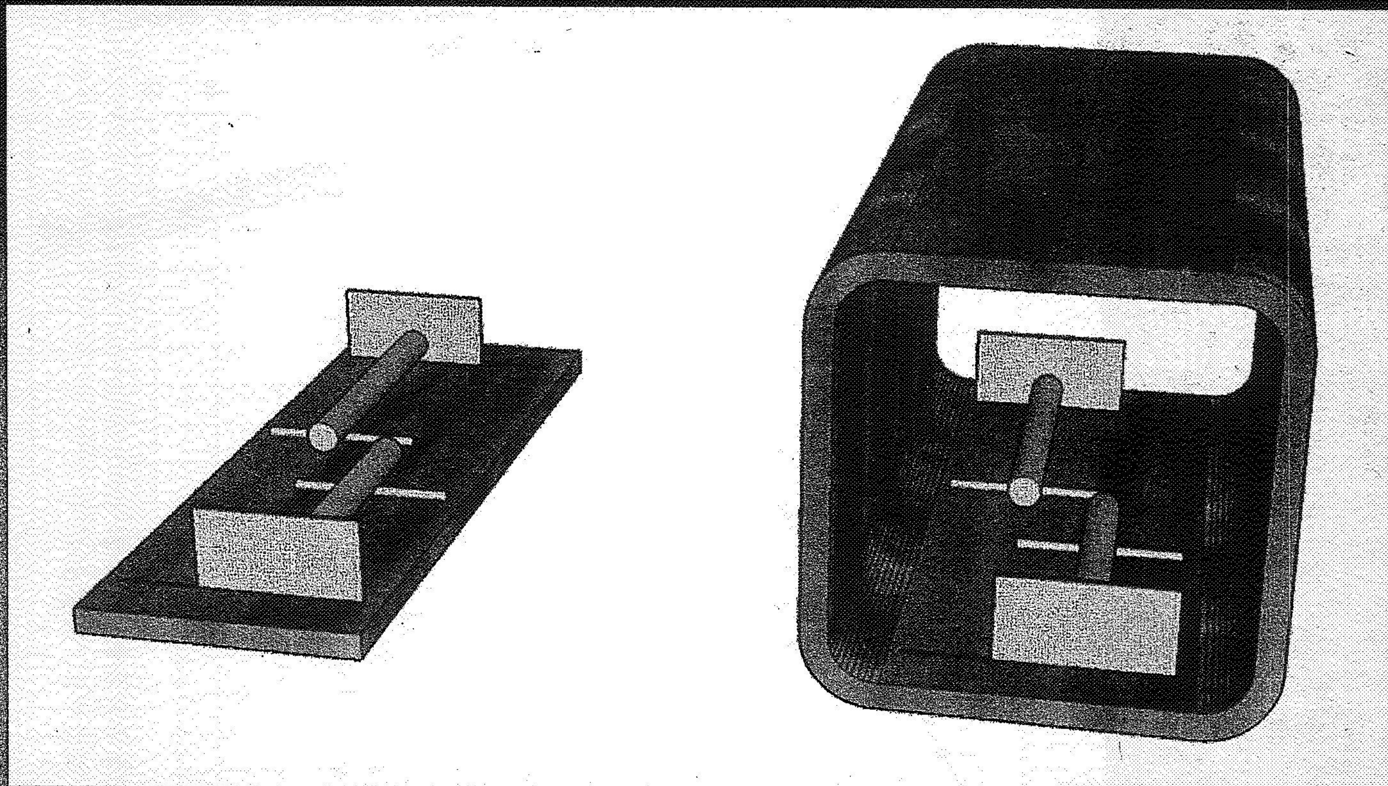

- Horizontal configuration
- Machined grooves
    - Interior
    - Single flat
    - 12.7 mm from each edge
    - Depth is < 0.1 mm

Thermal Expansion: Measurement Summary

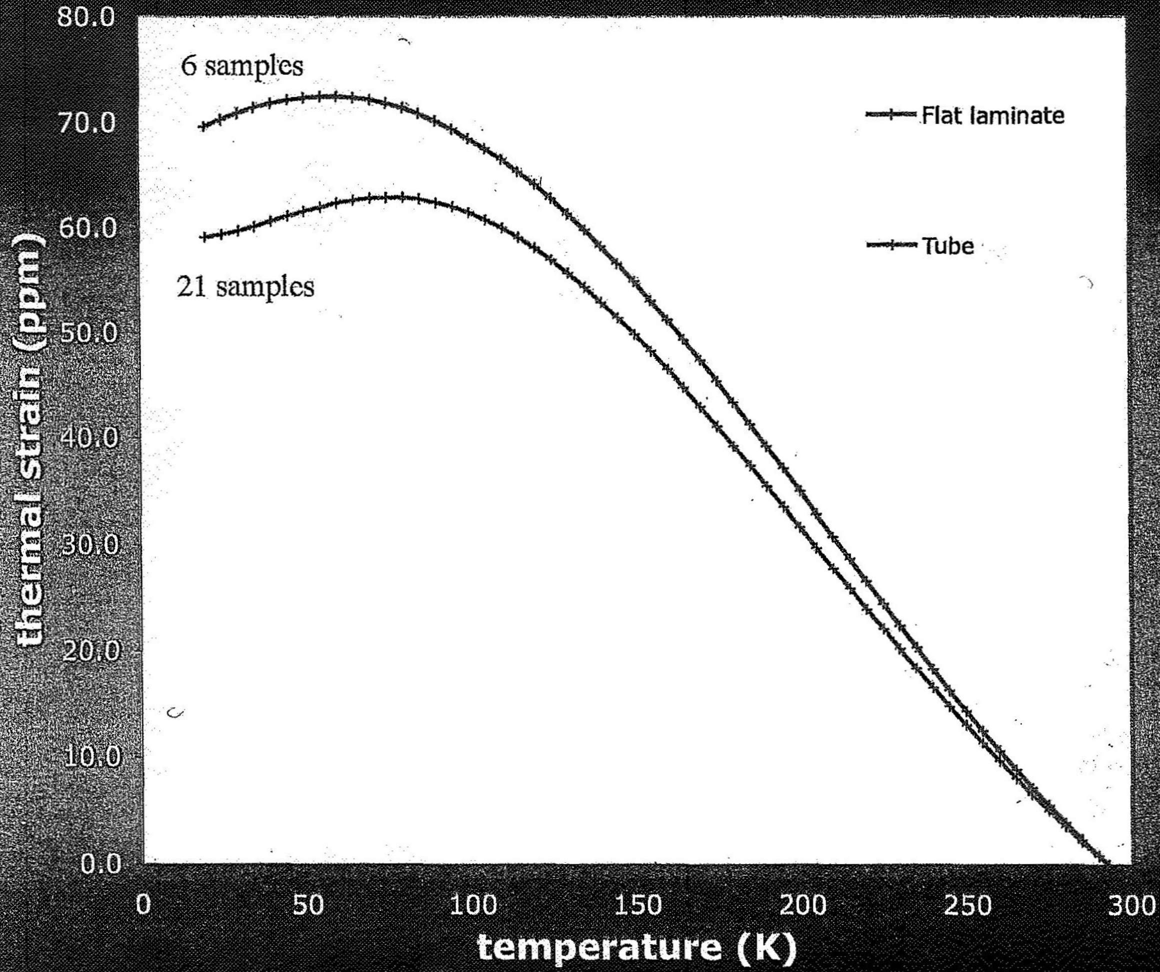

- Average responses are shown. Determined from the average of the best-fit polynomial coefficients (6th order) for individual samples.
- Tube has one extra ply on the inside of the tube. This will be included in the FEM comparison on the following charts.

Thermal Expansion: Examination of distorted shape from FEM

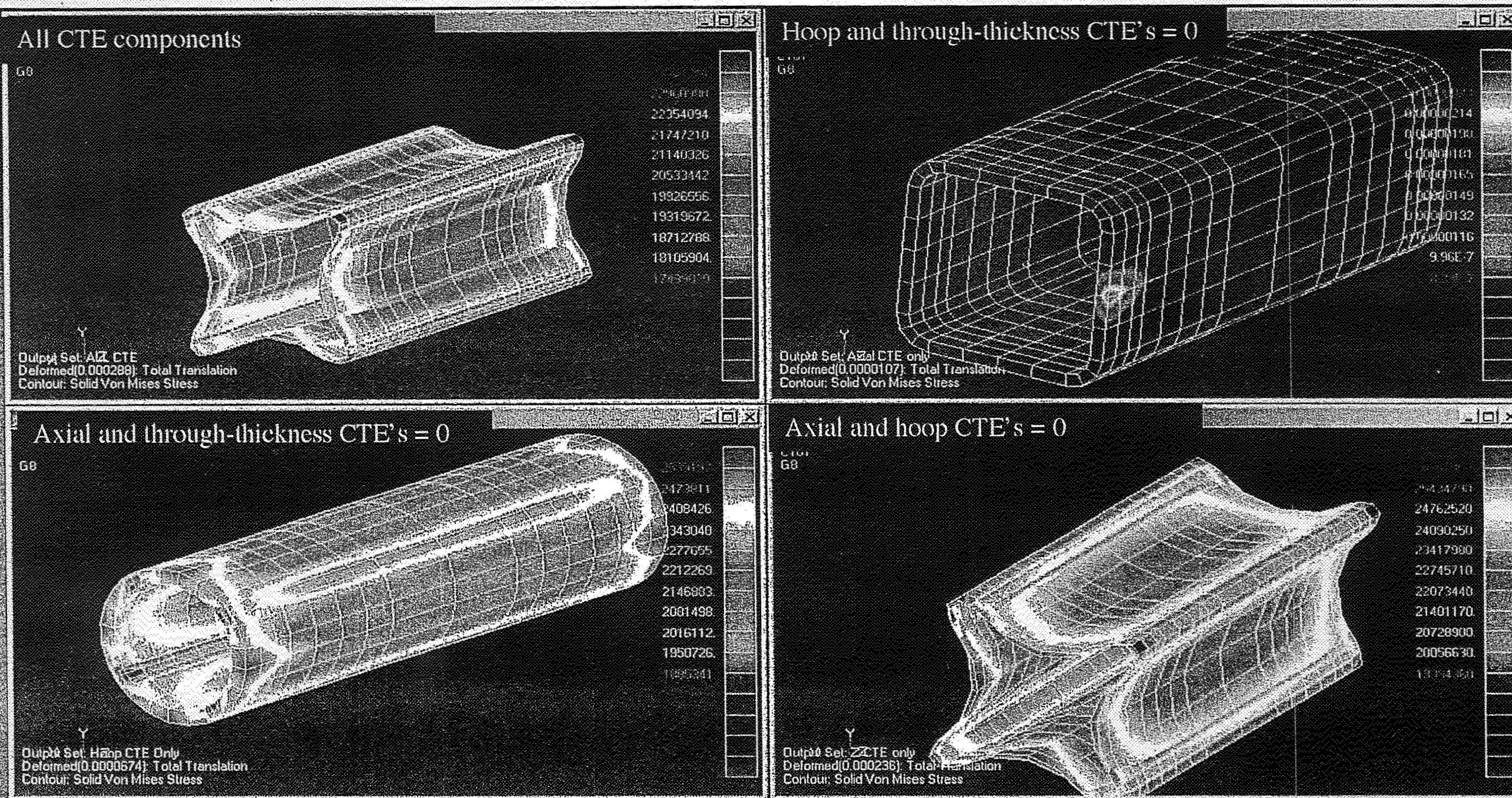

Tube thermal distortion due to bulk cool down is not stress free. Interactions between anisotropic material response and closed-from geometry result in characteristic "butterfly" cross-sectional change as well as edge effects.

Note: FEM coordinate system does not correspond to laminate coordinate system

Thermal Expansion: Predicted cool down strains FEM at 30K

Only axial displacement turned on for visualization.

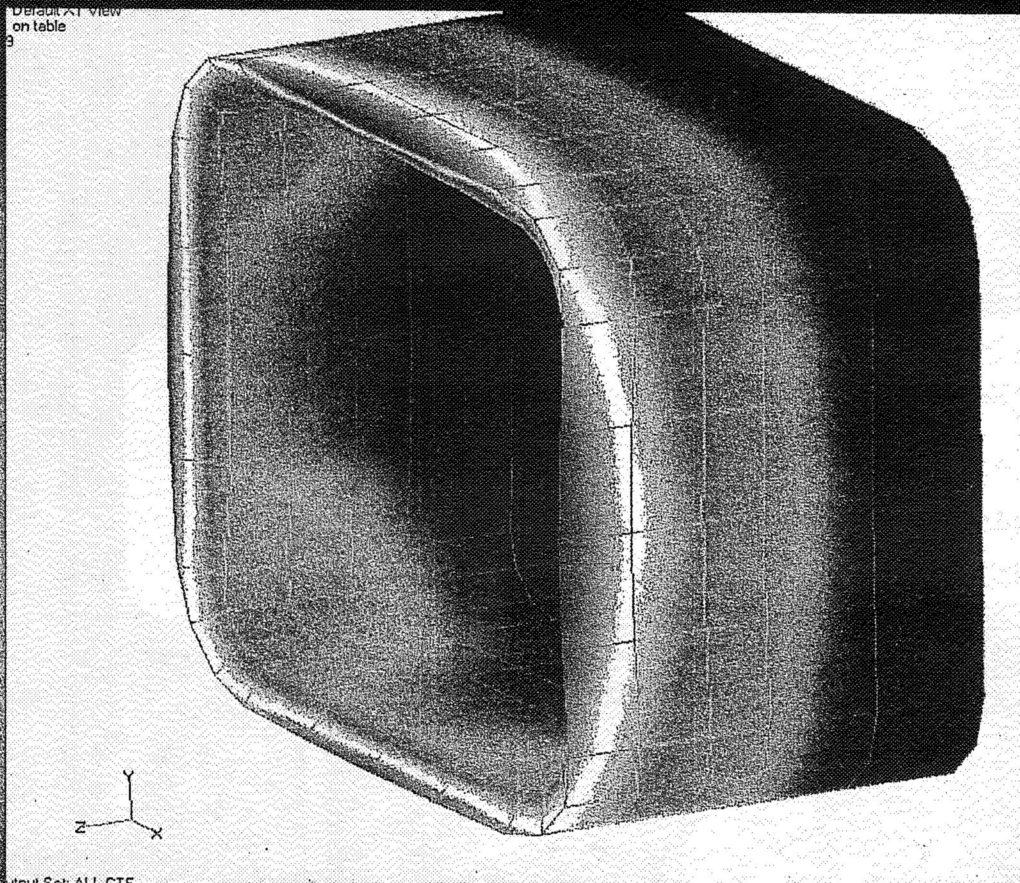

Axial Input:

$\alpha_{x,\,input} = \alpha_{x,\,flat}$ = -0.2694 ppm/K (Secant @ 30K)

$\varepsilon_{x,\,input} = \varepsilon_{x,\,flat} = \alpha_{x,flat}$ * (30K-293K) = 70.9 ppm

Recovered cool down strains at 30K:

End of tube all nodes

$\varepsilon_{x,end} = \varepsilon_{x,flat}$

End of tube, outer edge

$\varepsilon_{x,outer} = 1.18^* \varepsilon_{x,flat}$

End of tube, inner edge

$\varepsilon_{x,inner} = 0.80^* \varepsilon_{x,flat}$

Inside tube, 6.35 mm from edge

$\varepsilon_{x,6.35} = 0.84^* \varepsilon_{x,flat}$

Inside tube, 12.7 mm from edge

ε [illegible] = ε [illegible] = 0.87* ε [illegible]

Inside tube, 38.1 mm from edge

$\varepsilon_{x,38.1} = 0.98^* \varepsilon_{x,flat}$

FEA predicts that tube edge effects result in variation in measured thermal strain depending on measurement location.

Thermal Expansion: Reconciling Results

To compare tube and flat laminate results, $\varepsilon_{x,\ flat}$ must consider the extra T-300 ply found in the tube. Laminated plate theory is used to scale the two layups, where the cooldown strain ratio

$$\varepsilon_{x,[(60*/0\#/-60*/0\#)S8/0*]} / \varepsilon_{x,[(60*/0\#/-60*/0\#)S4]} = 0.97.$$

This gives the following relationship between tube and flat plate:

$$\varepsilon_{x,\ GSFC\ flat} = (\varepsilon_{x,\ GSFC\ tube}/0.87)/0.97$$

Adjustments using FEM and laminated plate theory reconcile the cool down strain measurements to within 1 ppm.

Capturing Materials Data: Motivation

1. JWST Needs:
   - Provide data and materials traceability for JWST Integrated Modeling effort.
   - Retrieve and connect test values to their original pedigree information.
   - Examine material variability in sensitivity studies.

2. Maximize Data Utility
   - Provide accurate cryogenic data to a wider community.
   - Facilitate higher level analysis, comparison, and selection of materials and properties.

3. Streamline basic requests
   - Direct others for "handbook" questions.
   - Connect multiple lab reports.

Capturing Materials Data: Example of Existing Data

http://cryogenics.nist.gov/NewFiles/Invar.html

Young's Modulus

Linear Expansion $[(L-L_{293})/L_{293}]\times10^5$

$x = a + bT + cT^2 + dT^3 + eT^4$ $\qquad T \Rightarrow T_{low}$

$x = f$ $\qquad T < T_{low}$

	Young's Modulus	Linear expansion
a	1.41565E2	-5.265E1
b	2.54435E-2	1.009E-1
c	-1.00842E-3	8.395E-4
d	6.72797E-6	-1.973E-6
e	-1.08230E-8	8.794E-11
T_{low} (K)		80
f		-40
data range (K)	1-298	4-300
equation range (K)	3-298	4-300
% error	1	5

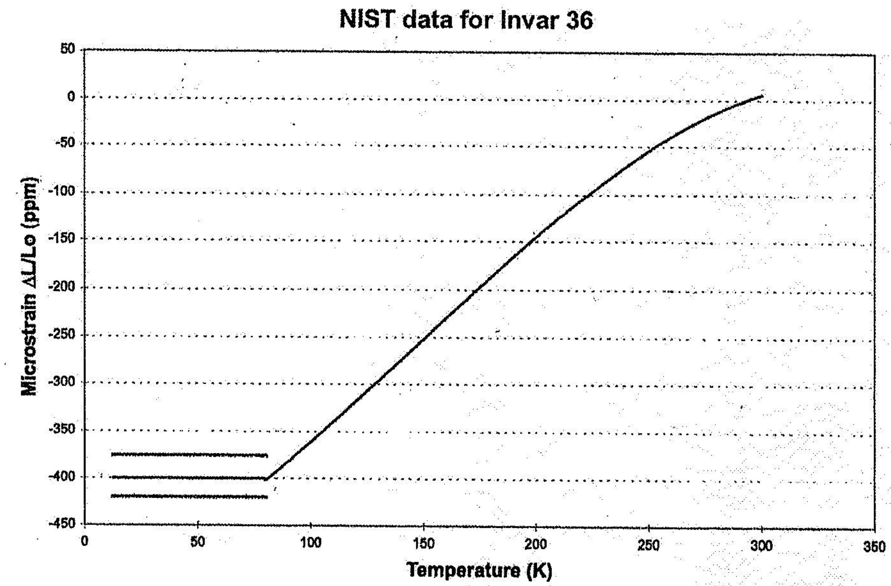

Material Properties

physical and chemical properties

Physical and Chemical Properties Division

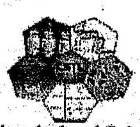

Chemical and Science Technology Laboratory

NIST Boulder Labs

NIST HOME

NIST Homepage

Capturing Materials Data: Database Setup

Materials Pedigree
contains relevant materials characteristics, such as chemistry, manufacturing specs, form, etc.

Work Request
contains standard info, such as project, date submitted, data completed, etc.

Test data
Contains summary of material tested and all test data

Test Equipment
Contains a description of the instrument that performed the measurement

Capturing Materials Data: Summary